ΕΘΝΙΚΟ ΜΕΤΣΟΒΙΟ ΠΟΛΥΤΕΧΝΕΙΟ

ΣΧΟΛΗ ΧΗΜΙΚΩΝ ΜΗΧΑΝΙΚΩΝ

ΔΙΑΤΜΗΜΑΤΙΚΟ ΠΡΟΓΡΑΜΜΑ ΜΕΤΑΠΤΥΧΙΑΚΩΝ ΣΠΟΥΔΩΝ

ΕΠΙΣΤΗΜΗ ΚΑΙ ΤΕΧΝΟΛΟΓΙΑ ΥΛΙΚΩΝ

ΕΡΓΑΣΤΗΡΙΟ ΤΕΧΝΟΛΟΓΙΑΣ ΑΝΟΡΓΑΝΩΝ ΥΛΙΚΩΝ

ΜΕΤΑΠΤΥΧΙΑΚΗ ΕΡΓΑΣΙΑ

Αξιολόγηση κεραμικών ηλεκτροδίων στην παραγωγή ενέργειας και αξιοποίηση αποβλήτου μέσω μικροβιακής κυψελίδας καυσίμου

Ιωάννα Καραμήτρου

Πτυχιούχος Τμήματος Χημείας Πανεπιστημίου Κρήτης

Α.Μ. 51122008

Επιβλέποντες: Δρ. Χρήστος Αργυρούσης, Καθηγητής ΕΜΠ

Δρ. Παύλος Κ. Πανδής, Επιστημονικός Συνεργάτης ΕΜΠ

ΑΘΗΝΑ 2024

NATIONAL TECHNICAL UNIVERSITY OF ATHENS

DEPARTMENT OF CHEMICAL ENGINEERING

INTERDEPARTMENTAL MASTER PROGRAM

MATERIAL SCIENCE AND TECHNOLOGY

LABORATORY OF INORGANIC MATERIALS TECHNOLOGY

MASTER THESIS

Evaluation of ceramic electrodes in energy production and waste utilization through microbial fuel cells

Ioanna Karamitrou

Graduate of the Department of Chemistry, University of Crete

R. N. 51122008

Supervisors: Dr. Christos Argirousis, Professor NTUA

Dr. Pavlos K. Pandis, Scientific associate NTUA

ATHENS 2024

Acknowledgments

The present research which was performed in the Laboratory of Inorganic Material Technology, was supervised by Prof. Christos Argirousis to whom I am grateful for his support and trust.

My sincere thanks to Dr. Pavlos K. Pandis, the co-supervisor of this work, who stood by me from the beginning till the end and taught me to work in a systematic manner and focus on the important things as required in research.

Last but certainly not least, I would like to express my gratitude to the people supporting me in numerous and various ways throughout the years, my parents, my sister and my friends, for being proud of whom I have become.

Table of contents

Abbreviations and acronyms

BOD	Biochemical Oxygen Demand
CE	Coulomb Efficiency
CLD	Constant Load Discharge
COD	Chemical Oxygen Demand
CV	Cyclic Voltammetry
MET	Microbial electrochemical technologies
MFC	Microbial Fuel Cell
ORR	Oxygen Reduction Reaction
OCV	Open Circuit Voltage

Abstract

The development of efficient and cost-effective Microbial Fuel Cells (MFCs) has the potential to revolutionize sustainable energy production by harnessing the metabolic processes of microorganisms to generate electricity from organic waste. This master's thesis presents the design, fabrication, and evaluation of two single-chamber MFCs, each featuring four air cathodes and an intricate electrode design aimed at maximizing surface area. Both MFCs were constructed using 3D-printed acrylonitrile butadiene styrene (ABS) polymer reinforced with carbon, chosen for its affordability and mechanical properties.

The study involved two distinct configurations: the first MFC had its cathodes and anode treated solely with sodium hydroxide (NaOH), while the second MFC received the same NaOH treatment with the additional enhancement of manganese dioxide (MnO_2) coating on the outer side of its cathodes. Prior to applying the MnO_2 coating, extensive testing was conducted on the ABS-C material using both acetone and NaOH treatments to evaluate their effectiveness in improving the material's bio-compatibility and electrochemical properties. Results indicated that the NaOH treatment was superior, effectively preparing the material for microbial colonization and enhancing its electrochemical performance.

Following the inoculation of the anodes with an appropriate microbial consortium, each MFC underwent three operational cycles. Measurements were meticulously recorded, focusing on open circuit voltage (OCV), polarization and power curves, as well as COD (chemical oxygen demand) reduction during each cycle. The performance comparison revealed a significant improvement in waste treatment, power generation and current intensity for the MFC with MnO_2-coated cathodes compared to the MFC treated only with NaOH.

The intricate 3D-printed designs of the electrodes contributed substantially to the overall performance by providing an increased surface area for microbial attachment and electrochemical reactions. This structural advantage, combined with the MnO_2 catalyst's enhancement of the cathodic reactions, underscores the importance of both material treatment and electrode design in optimizing MFC performance.

This research demonstrated the viability of using inexpensive, readily available materials like ABS polymer reinforced with carbon in the construction of MFCs, provided they are properly treated and optimized for electrochemical applications. The findings suggest that the combination of NaOH treatment and MnO_2 coating significantly boosts the efficiency of MFCs, paving the way for more effective and scalable microbial fuel cell technologies.

The outcomes of this study offered valuable insights into the design and enhancement of MFCs, highlighting the critical role of electrode surface treatments and catalytic coatings in achieving higher power densities and more efficient energy conversion.

1.1.1 Microbial Fuel Cells

The overexploitation of fossil fuels and their adverse effects on the environment have raised serious concerns. These include greenhouse gas emissions, ozone depletion, global warming, and the renewability of these resources. Consequently, alternative sources of energy must be sought. [1]

Microbial fuel cell (MFC) technology has received increasing attention due to the high demand for sustainable energy and fresh water. During the last 40 years, extensive research and concerted efforts have led to significant technological advances, increasing capacity and understanding. The power output of a single MFC unit has seen expanding growth, and some researchers claim that laboratory-scale MFCs can already achieve sufficient current density for practical applications. [2]

Biodegradable waste and pollution make renewable energy readily available. The use of wastewater as biofuel not only provides energy, but also helps in waste processing and disposal. Microbial fuel cells (MFCs) are devices that simultaneously treat wastewater and generate electricity. [3] MFCs use microorganisms to oxidize organics that degrade in an anaerobic anode chamber, producing bioelectricity through the production of electrons and protons, which are then transferred to the cathode chamber. [4]

Therefore, the technology of MFCs, as the basis of biological wastewater treatment systems, is a worthy proposition to modern challenges, since it offers solutions both in the reduction of organic load in wastewater and in the production of clean electricity. However, despite significant developments over the last decades, the commercial exploitation of the MFC technology has been delayed due to several inhibiting factors, such mostly low electrical power efficiency, high material costs, including the high price of Proton Exchange Membrane (PEM), as well as expensive metal catalysts used in the electrodes. Up to this date, several researches have been carried out to enable this technology to be used in real-world applications. [5]

In order to enable bio-electrochemical treatment of wastewater, the cost of the materials used in MFCs should be reduced. The cathodes in MFCs represented the largest share of the total capital cost, while the surface area and the material they are made of contribute significantly to electrical power production. For this reason, it is important to identify low-cost materials, as well as cathode architectures in order to improve the efficiency and performance associated with the removal of the organic load of the wastewater and the generation of electrical power. [6]

1.1.2 Principal operation of MFCs

MFC is a tool that uses the catabolic activity of microorganisms to generate electricity from organic matter. [7] At the anode, organic matter is oxidized by electrochemically active microorganisms and electrons being released. The generated electrons are then transferred to the cathode via an external circuit and electricity is generated. [8] Numerous models have been designed for MFC, but they can be divided into two categories, dual-chamber, and single-chamber (Figures 1 and 2).

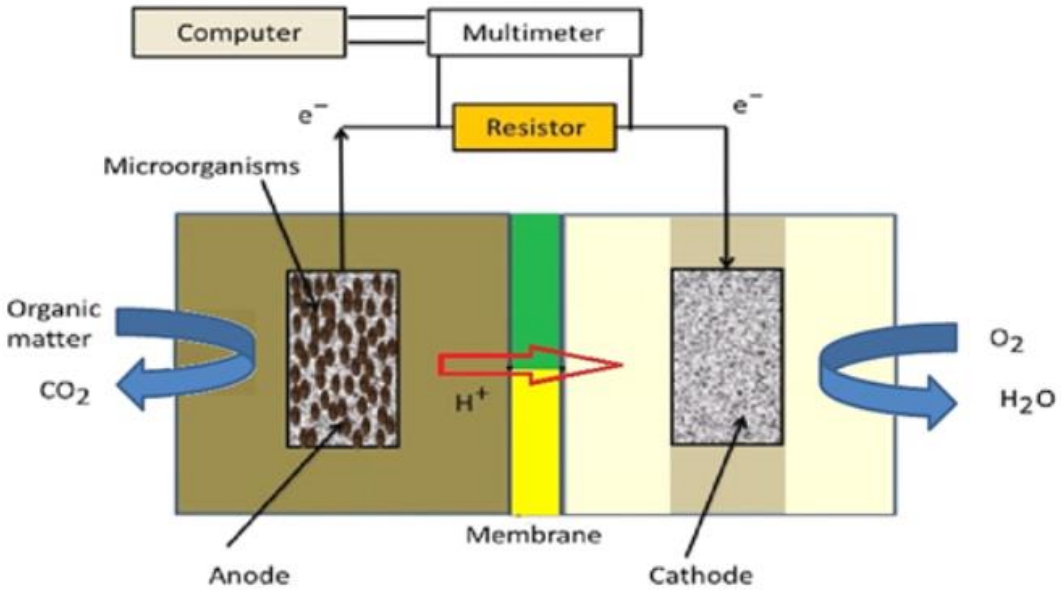

Figure 1: *Schematic diagram of two-chambered MFC [9]*

Dual-chambers include an anaerobic anode chamber and aerobic cathode chamber, which are separated by a proton exchange membrane (PEM). The substrate is oxidized as a fuel by microorganisms in the anaerobic chamber in which the anode electrode is located, and electrons and protons are released. Protons transfer to the cathode chamber through the proton exchange membrane, protons and electrons react with oxygen to form water in the cathode chamber. For instance, the following reactions show the oxidation of acetate at the anode and the reduction of oxygen at the cathode. [9]

$$CH_3COO^- + 2H_2O_2 \leftrightarrow CO_2 + 7H^+ + 8e^-$$

$$O_2 + 4e^- + 4H^+ \rightarrow 2H_2O$$

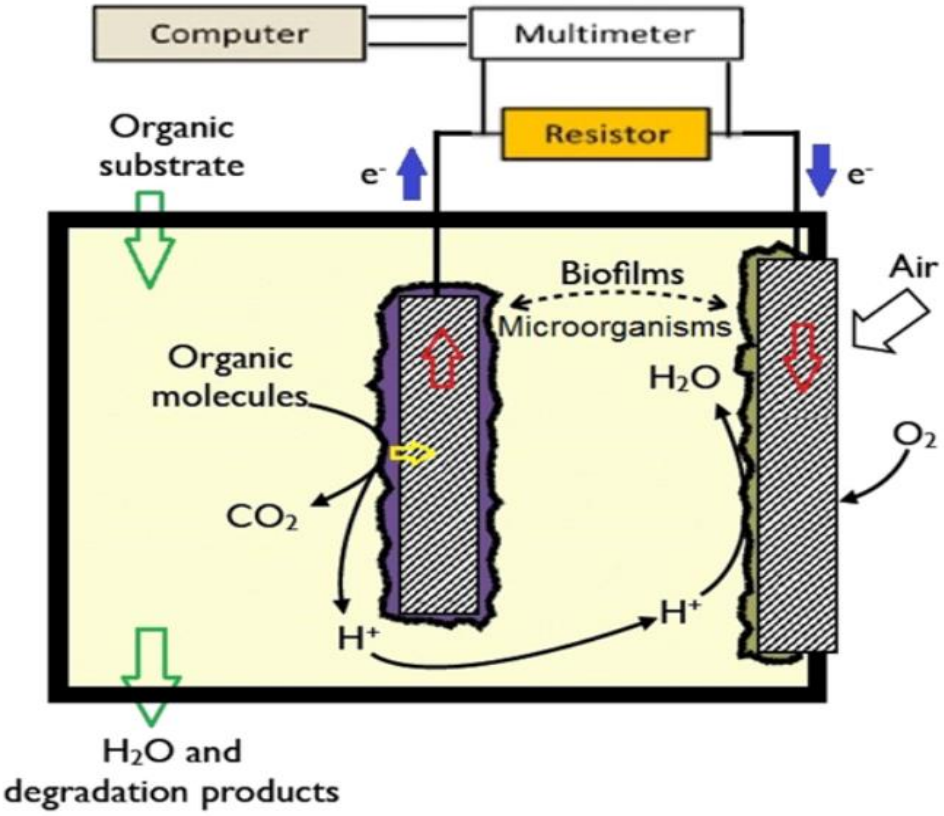

Figure 2: *Schematic diagram of* single-*chambered MFC*

In a single-chamber system, as in Figure 2, the cathode and PEM chambers have been removed; therefore, it has a simpler design and more affordable price. The cathode is exposed to air on one side and water on the other side (inside). Anodic reactions are similar to a dual-chamber system and oxygen in the air can directly react at the electrode.

1.1.3 Operating conditions of MFCs

The operation of a MFC is influenced by several physicochemical parameters that affect bacterial growth and biofilm formation, consequently impacting the overall performance of the MFC. These parameters include pH, temperature, and the concentrations of substrates and ions.

pH: The effect of anodic pH on the performance of MFC systems has been extensively researched. It has been observed that, in most cases, the optimal pH is around 7 (neutral) or within a close range (6-8). The operation of NIR systems under extreme pH conditions has rarely been reported. Although several factors, such as ion

transport, substrate oxidation, and oxygen reduction, influence pH during the operation of microbial electrochemical systems, their effects can be mitigated through the use of appropriate catalysts, ion exchange membranes, and the addition of buffers. Additionally, the pH of the electrolyte directly affects the growth and viability of bacterial communities, as microorganisms are highly sensitive to their surrounding environment. Even slight variations in pH can lead to significant changes in cellular metabolism. [10]

Temperature: Microbes are highly sensitive to temperature, making the optimization of microbial biofilm growth and electrocatalytic activity dependent on the operating temperature. Bacteria can be categorized into three groups based on their preferred growth temperature: psychrophilic (<15°C), mesophilic (15-40°C), and thermophilic (>40°C). Most MFCs operate within the mesophilic range, indicating that the majority of electrochemically active bacteria function optimally at mesophilic temperatures. However, there are instances of psychrophilic and thermophilic bacteria exhibiting electrochemical activity. In microbial fuel cells with mixed microbial cultures, temperature dictates the nature and distribution of microbial communities, as each species has a distinct optimal growth temperature. Additionally, temperature variations alter the kinetics and thermodynamics of anodic reactions, which indirectly affect biofilm growth. [10]

Substrate: A wide variety of substrates have been utilized in MFC applications, ranging from simple compounds to complex mixtures of organic substances. Pure substrates that have been employed include glucose, acetic acid, butyric acid, lactic acid, proteins, cellulose, cysteine, glycine, and glycerol. Among various complex organic substrates, wastewater has proven to be a viable, nutrient-rich medium suitable for MFCs. The concentration of the substrate is also a critical factor. Studies have shown that increasing the substrate concentration from 100 to 850 mg/L can elevate the output power density from 0.2 to 1.2 W/m^3. However, at concentrations between 1000-1500 mg/L, the output power remained unchanged. Moreover, at higher substrate concentrations, a decrease in power density has been observed, attributed to substrate inhibition, which creates unfavorable conditions for biofilm growth and metabolism. [11]

Ion Concentration: The conductivity of the solution in a MFC is a critical factor that determines the rate of ion transport. Higher ion concentrations enhance ionic conductivity and reduce ohmic losses, thereby increasing the output power of the MFC. Conductivity is typically increased by adding NaCl or a high concentration buffer solution. However, it has been reported that very high salinity can negatively impact bacterial growth. Therefore, when adding any component to improve ionic strength and thereby enhance MFC performance, it is essential to consider its potential effects on biofilm growth. [12]

1.1.4 Microorganisms used in MFCs

Most MFCs use wastewater as a power source. In open systems based on the sediment occurs selection electrogenic communities. Such consortia in the anode chamber should have functions similar to the communities of methanogenic anaerobic digesters, except that microorganisms capable of transferring electrons to the electrode replace methanogens. Such microbiocenoses are called anodophilic. In systems in sediments from 50 to 90% of the microorganisms at the anode are G-Proteobacteria. To a lesser extent Cytophagales (to 33%), Firmicutes (11.6%), J-Proteobacteria (9-10%). This fact indicates that the uniqueness of the community in open systems depends on the type of sediment. For example, freshwater microorganisms from Geobacteraceae are responsible for freshwater sediments. On the other hand, the high representation of Geobacteraceae (G-Proteobacteria) in anodophilous communities with different types of substrates (bottom sediments) is not surprising. Geobacteraceae are the predominant microorganisms in various sedimentary environments in which the reduction of Fe (III) oxide is the main terminal electron-acceptor process. Microorganisms-electrogenes can utilize a wide range of substrates, depending on the species. For example some species have the ability to produce a current in the presence of glucose as a substrate – Saccharomyces sp., Escherichia coli, Proteus vulgaris, Clostridium beijerinckii, Clostridium butyricum. [9]

1.1.5 Mechanism of electron transfer

A key process in MFCs is the transfer of electrons from the inside of a microbial cell to the outside environment due to the inability of solid electrodes to pass through cell walls. The requisite condition is either attained by using membrane-bound redox enzymes for aiding electron transfer out of cell or by direct physical transfer of reduced substances.

Regardless of the mechanism, electron transfer to the electrode targets redox-active entities that create an electrical connection between the bacterial cell and the electrode. These entities, commonly known as "mediators," include outer-membrane redox proteins, soluble redox shuttles, or reduced primary metabolites.

To maintain physical contact with the electrode surface, mediators have to exert electrochemical activity in them at a definite electrode. At the same electrode surfaces, oxidation overpotential has to be low.

The linking species can be classified as either membrane-bound or soluble compounds. Electron transfer mechanisms are broadly categorized as direct electron

transfer (DET) using membrane-bound redox proteins or pili without any dissolved species, and mediated electron transfer (MET) with mediators involved. [13]

Direct Electron Transfer Mechanism

Exoelectrogens are microorganisms that directly transport electrons produced from the oxidation of organic matter to the anode in microbial fuel cells (MFCs) using bacterial membrane-redox-active proteins, including multi-heme proteins and c-type cytochromes, as well as pili. [14]

Sveral exoelectrogens have reported to employ DET mechanism for transferring electrons to the anode but Geobacter sulfurreducens is the most extensively studied in this regard also because its genome has been sequenced. It is reported that about 110 genes in the G. sulfurreducens genome code for assumed c-type cytochromes anticipated playing a pivotal role in extracellular electron transfer. [15]

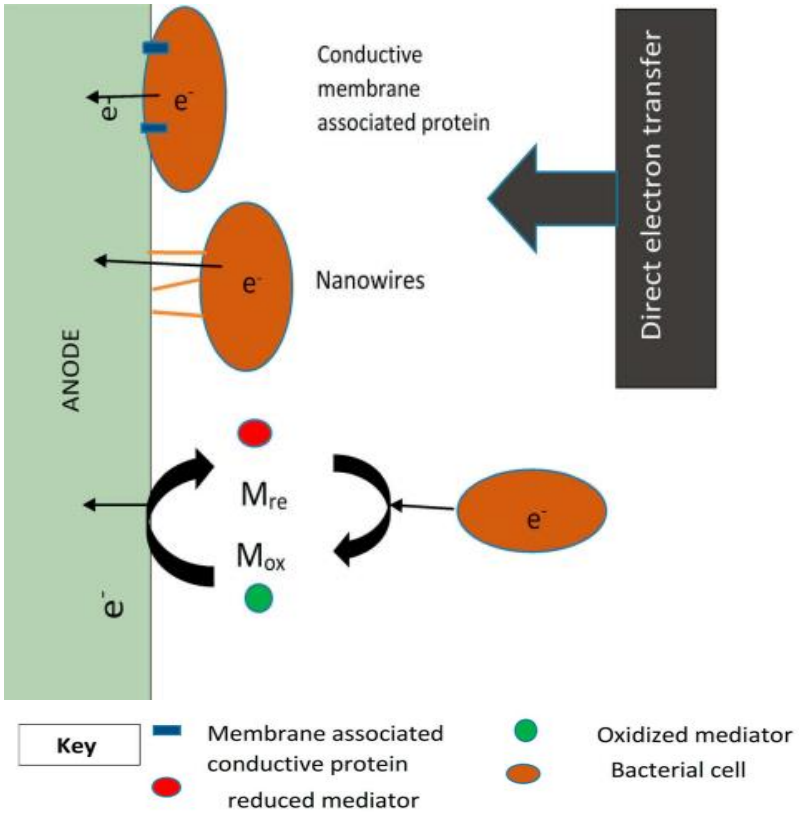

Figure 3: *Schematic representation of the direct electron transfer mechanism in a microbial fuel cell [10]*

1.1.6 Biofilm formation

The formation of a thick biofilm attached to an impermeable substratum e.g. graphite block is a crucial for the optimal function of the MFCs. Biofilms thicker than 20–50 μm are most likely to be diffusion limiting and stratified. Feedstock substrates diffuse into the biofilm, but outer layers of cells will utilize the substrate leaving less for the inner layers. This gives rise to the formation of gradients for both the end terminal electron acceptors (e.g. oxygen) and carbon-energy substrates. Both gradients go from the outside to the inside. In addition, the biofilm matrix fluid has a long replacement time and the mean growth rate of the total biofilm is slow. Inner cells may be close to starvation and trying to survive rather than grow. This gives rise to erosion due to layers of inactive cells whilst cells in the outer layers grow fast. It is probable that aerobes have majority towards the outside whilst anaerobes have majority deep inside with facultative species being distributed throughout. [16]

Biofilm attachment and detachment processes

When sterile surfaces are immersed in an aqueous medium containing protein, these molecules (but not cells) adhere quickly to the surfaces within seconds. In addition to the composition of the initial adhesion monolayer, surface conditioning could have an impact on which types of bacteria colonize the surface thereafter. [16]

The initial attachment of cells to a solid surface is characterized by several forces and their interactions: the advective flow and three non-covalent interactions Lifshitz-van der Waals or electrodynamic, Lewis acid-base, and electrical double layer. These interactions along with each free energy are analyzed and calculated by the extended DLVO theory (DLVO stands for Derjaguin, Landau, Verwey, Overbeek). [17] Furthermore, ionic bridges can be formed by divalent metal ions between negatively charged molecules or particles. Cell motility, generally conducted by flagella, can steer cells along concentration gradients, electric fields, magnetic fields, and light. [18] When it comes to mixed-species communities, pioneer species' existence on a surface increases the number of available binding sites for a second or following species. Many variables impact cell attachment and biofilm formation, including the type of substrate, its texture, roughness, and hydrophobicity, as well as the conditioning layer. Another factor that plays an important role are the properties of the cells, such as flagella, pili, fimbriae, capsules, and/or slime formation. Lastly the bulk fluid's properties, such as nutrient types and concentrations, pH, redox potential, divalent metal ions, oxygen, inhibitors, and temperature, are also important factors. [16]

Biofilm detachment occurs through distinct mechanisms such as erosion and shearing, where small portions of the biofilm are continuously removed. Other methods include sloughing (rapid and significant removal), abrasion (detachment caused by particles in the bulk fluid striking the biofilm surface), and natural shedding. These processes can impact the phenotypic traits of organisms. Erosion and sloughing are most commonly

seen in thicker biofilms found in nutrient-rich environments. The detached aggregates often retain biofilm characteristics like extracellular polymeric substances (EPS) and antimicrobial resistance properties, while naturally shed cells may quickly revert to a planktonic state.

Erosion from the biofilm tends to increase with greater biofilm thickness and higher fluid shear at the biofilm-bulk liquid interface. Sloughing is more unpredictable than erosion and is thought to result from nutrient or oxygen depletion within the biofilm. At high hydrodynamic shear rates, hard mineral particles in the input medium can remove biofilms through abrasion. [19]

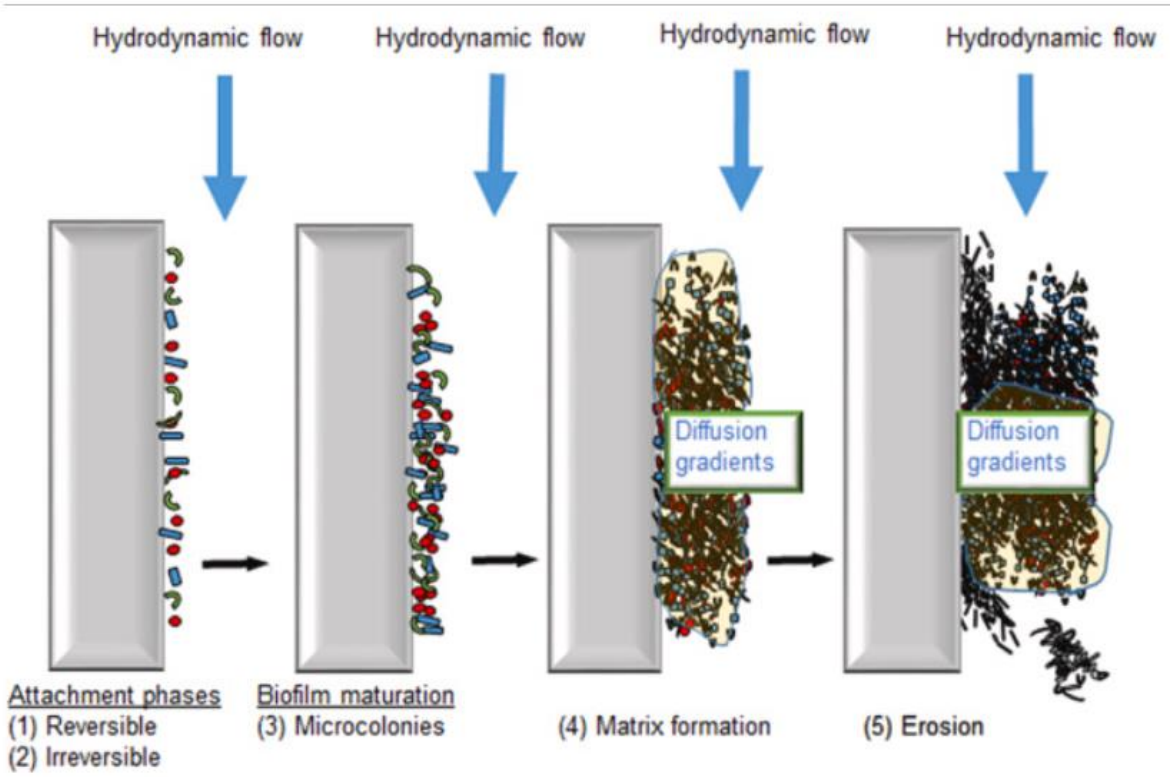

Figure 4: *Conventional example of biofilm indicating the attachment phase (1) and (2), biofilm maturation forming microcolonies (3), then matrix formation (4) and erosion (5)[13]*

1.1.7 3D Printed materials used in MFCs

In the past 20 years, microbial electrochemical technologies (METs) have proven successful in areas such as bioenergy generation, environmental monitoring, resource recovery, and producing platform chemicals. However, scaling up and commercializing these technologies remains difficult. Challenges include costly and complex fabrication processes, long start-up times, and intricate design needs, especially for large-scale systems. Recently, three-dimensional printing (3DP) has become a promising method for creating METs at the bench scale. It allows for low-cost, fast fabrication of complex and miniaturized designs, which traditional methods struggle to achieve. Using 3DP technology holds great promise for optimizing and scaling up METs. It can also help with the rapid start-up of bioanodes for current generation, reducing potential delays. [20]

Reactor Body

Most METs are designed for water and wastewater treatment, so the design of the reactor can greatly impact flow dynamics and as a result the performance of the cell. This makes it important to optimize aspects such as reactor shape, working volumes, and the placement of fluid inlets and outlets. [21] For example, a drop-like reactor shape may perform better than a square shape because it offers a larger effective surface area. [22] Additionally, including baffles in the anode chamber can lead to higher voltage output in microbial fuel cells (MFCs) by minimizing areas with slow flow rates. [23] However, creating these complex reactor designs can be challenging with traditional manufacturing methods, especially for miniaturized METs. Many studies have successfully used 3D printing for precise fabrication of reactor bodies for METs. [21] While 3D printing can enable the bulk production of small-scale reactors for biosensing applications in reasonable time and at a lower cost, direct 3D printing of large-scale systems is still not feasible. Nonetheless, combining 3D printing with computational fluid dynamics modeling (CFD) can facilitate cost-effective, advanced reactor engineering for large-scale MET applications, such as wastewater treatment. By using CFD modeling combined with 3D printing, lab-scale prototypes can be employed for the design and optimization of larger systems. [24]

Electrodes

The development of electrodes that possess highly porous structures for optimal bacterial adhesion and excellent electrochemical performance for high current output has been of great interest to the MET research community. Complex macro-porous 3D electrode materials have proven effective in providing larger surface areas for biofilm growth, thereby enhancing the electrochemical capabilities of microbial electrochemical technologies (METs). However, creating such complicated electrode designs using traditional methods is challenging. [25]

Recently, 3D printing has enabled rapid prototyping of ideal MET electrodes. For example, 3D printing allows for the precise creation of porous, X-shaped skeleton electrodes using materials like titanium and stainless steel. Further modification with polyaniline can create crumpled, biocompatible surfaces. Polyaniline-coated 3D-printed titanium electrodes have been shown to significantly increase power density compared to uncoated ones. [26]

Another study developed a 3D-printed aluminum alloy anode that generated energy output of up to 3 kWh/m^3 per day from a microbial fuel cell. The 3D microporous coral skeletal structure provided excellent surface roughness and biocompatibility for the electroactive microbes. However, metal 3D printing remains highly expensive, and some metal alloys used for printing may be prone to corrosion. [26] [27]

Polymeric materials such as polylactic acid (PLA) and UV-curable resin have also been explored for 3D printing electrodes for METs. Yet, the electrochemical performance of 3D-printed polymeric electrodes can be insufficient. For instance, one study found that power generation from a PLA electrode was significantly lower than from a plain carbon veil electrode with the same geometric structure. [27]

To address these issues, researchers have proposed techniques such as carbonization of 3D-printed polymer resin anodes to enhance biocompatibility and power density. Similarly, modifying 3D-printed polymeric electrodes with copper can result in a substantial increase in power output compared to copper mesh electrodes. [28]

Recently, a 3D-printed graphene oxide (GO) aerogel anode was developed using a customized printing ink that included GO, ferric ions, and magnetite nanoparticles. The hierarchical pores in the GO aerogel electrode facilitated effective mass transfer, leading to a significant increase in volumetric current output compared to carbon felt anodes. [29]

Overall, 3D printing for electrode fabrication has shown great potential. While researchers prioritize cost and performance, ensuring the long-term stability of 3D-printed electrodes, such as chemical stability and corrosion resistance, is crucial for them to be completely efficient.

Bioelectrodes

In addition to electrodes and other physical aspects of microbial electrochemical technologies (METs), the performance of these systems heavily relies on electroactive microorganisms. Selecting and cultivating efficient electroactive bacteria (EAB) can be challenging, as their slow growth rates mean it can take a long time (months or even years) to fully develop biofilms on anodes or cathodes, which in turn delays reactor start-up times. [30]

One approach to speed up biofilm enrichment involves using effluent from MET reactors as an inoculum source. However, a more innovative method for rapid biofilm development is still needed. A recent study proposed that 3D printing could provide a promising solution for these time-consuming biofilm development processes. The study used 3D printing to create a bioanode with living inks containing *Shewanella oneidensis MR-1*. Remarkably, the bacteria survived the 3D printing process, and the microbial fuel cell (MFC) produced a stable current for nearly 93 hours. [31]

Before this, 3D printing had been used to engineer objects and structures with various microorganisms such as Escherichia coli, Pseudomonas putida, Acetobacter xylinum, and yeast cells. [32] Due to the cells' adhesion during the process, 3D-printed objects with microbes can achieve high cell densities. These recent studies demonstrated the potential of 3D-printed bioanodes, which could open up new possibilities for high-performance METs. [32]

1.1.8 Liquid waste

Liquid waste is the residues of everyday activities in liquid form, such as domestic, industrial and agricultural wastewater. The sediment resulting from wastewater treatment processes is called sludge and is the solid part of wastewater. Liquid waste, based on its source of origin, is divided into:

- Domestic wastewater, which includes runoff from domestic, commercial and municipal water uses. They originate from daily activities related to cooking, cleaning, use of baths, laundry and toilets.
- Industrial wastewater, originating from industrial activity and depending on the type, extent and characteristics of the activity.
- Stormwater, which enters the drainage system in various ways.
- Water from storms and precipitation in general. [33]

Over the last century, population growth and industrialization have led to the degradation of ecosystems that sustain human life. In aquatic ecosystems, this is largely due to the discharge of untreated industrial and urban wastewater. To address this growing threat, government bodies are implementing stricter regulations focused on waste reduction. Meeting these regulatory obligations often increases capital and operating costs for waste treatment systems, creating a financial burden on industries. However, compliance with environmental regulations can offer secondary revenue sources rather than just additional costs.

Biological treatment of wastewater is more cost-effective and avoids causing secondary pollution compared to other methods. This approach began in the late 19th century and has evolved from passive disposal to resource utilization. This shift has

been gradual, allowing traditional methods to coexist with new biotechnology-based approaches.

Biodegradation methods focus on eliminating organic matter and nutrients using microorganisms. These microorganisms break down nutrients, colloidal, and dissolved organic matter, and excess microorganisms are removed from treated wastewater through natural processes. Biodegradation can occur under either aerobic or anaerobic conditions, depending on the microorganisms used. Aerobic technologies are typically applied for treating wastewater from smaller sources. However, the high energy costs of providing oxygen have driven research toward new, more energy-efficient technologies.

Anaerobic reactors, primarily used in industrial wastewater treatment, are also common in municipal wastewater treatment. Large-scale anaerobic systems offer a cost-effective approach for domestic wastewater treatment due to lower construction, operation, and maintenance costs, minimal sludge production, and the benefit of biogas production.

Despite the advantages of anaerobic treatment, wastewater must then be further treated to remove residual organic load, nutrients and pathogens in order to meet the emission standards in most countries. [34]

Determination of organic load in wastewater

Biological processes, which involve removing most organic components from wastewater through biological oxidation, are used during secondary treatment, after primary treatment. These methods rely on the growth of specific microorganisms in a controlled environment, which consume the organic load as a substrate for their growth. Laboratory tests like Biochemical Oxygen Demand (BOD) and Chemical Oxygen Demand (COD) measure the organic content in wastewater at concentrations greater than 1 mg/L. The most common measure is BOD, which gauges the Dissolved Oxygen (DO) needed for biochemical oxidation of the organic matter in waste according to the overall reaction:

$$Organic\ Matter + DO\ Microbial\ cells \rightarrow CO_2 + H_2 + NH_3 + ... + new\ cells$$

BOD measurements are used for several purposes:

- Estimating the oxygen needed to biologically stabilize organic matter
- Determining the size of wastewater treatment plants
- Assessing the efficiency of some processes
- Checking compliance with legal limits for treated wastewater released into the environment

As an alternative to BOD, the organic content can be assessed using the COD parameter, which measures the amount of a specific oxidant that reacts with the wastewater sample under controlled conditions. The oxidant consumed is then equated to the equivalent amount of oxygen. The dichromate ion ($Cr_2O_7^{2-}$) is commonly used as the oxidant because it reacts with the sample and is reduced to trivalent chromium (Cr^{3+}). Methods such as the Open Reflux and Closed Reflux Colorimetric techniques use COD measurement. Both organic and inorganic components of a sample undergo oxidation, but the organic portion is typically more significant and of greater interest. [35]

1.1.9 Electricity generation and energy recovery

Electrical production

An MFC typically produces an operating voltage (V) of about 0.5V, which is a function of the external resistance (R_{ex}) and current I, according to the relationship:

$$V=I*R_{ex}$$

The highest voltage is produced in open circuit mode and is referred to as Open Circuit Voltage (OCV). The theoretical maximum voltage that can be produced by a MFC is limited by thermodynamics and can be predicted by the Nernst equation. This is of the order of 1.1 V.

The output power of the MCC is calculated from the product of the measured voltage and the generated current:

$$P=I*V$$

To evaluate the output power produced by an NPP, the power density is calculated based on the electrode surface area or the volume of the bioreactor. The surface power density is the output power normalized with the electrode surface:

$$\mathbf{P_a}=\frac{P}{Ac} \qquad \mathbf{P_c}=\frac{P}{Aa}$$

in which P_a and P_c are the power density based on the surface area of the anode and cathode, respectively. A_a and A_c are the effective areas of the anode and cathode, which can be either the specific or geometric surface area. Also, in a membrane-based MFC, the power density may be proportional to the membrane surface area. Based on the volume of the bio-reactor (V_R) of an MFC system, the volumetric power density (P_V) is defined, expressed as follows:

$$\mathbf{P_V = \frac{P}{VR}}$$

Energy recovery

The aim of MFC technology is to recover the energy contained in the wastewater. Coulomb efficiency (CE), defined as the fraction of the electrical charge (Coulombs) recovered relative to the total energy contained in the wastewater, is used to evaluate the electron recovery efficiency from the wastewater:

$$\mathbf{CE = \frac{electrical\ charge\ recovered\ (Coulombs)}{Total\ charge\ of\ substrate\ (Coulombs)}}$$

The electric charge is calculated by integrating the electric current with respect to time, so the Coulomb yield, using COD as a measure of the substrate concentration, is expressed as follows:

$$\mathbf{CE = \frac{8 * \int_t^0 I dt}{F * VR * \Delta COD}}$$

where:

8: a constant obtained as the ratio of the molecular weight of oxygen (32g/mol) to the number of electrons (4) exchanged per mole of oxygen.

F: the Faraday constant

V_R: the volume of the bioreactor (anode chamber)

ΔCOD: the change in COD of the substrate with time t [36]

1.2 Current work

The current work focused on evaluating the viability of using a cost-effective, 3D-printed ABS polymer reinforced with carbon in the electrode construction of microbial fuel cells (MFCs) for wastewater treatment and energy generation. Both anode and cathode were 3D printed whilst cathode underwent two different configurations. Anode was treated with NaOH and cathode was treated firstly with sodium hydroxide (NaOH) and secondly a MnO_2 coating was applied onto the already treated cathodes. This study aimed to demonstrate the effectiveness of the treated 3D polymer in achieving substantial chemical oxygen demand (COD) reduction and enhanced electrochemical performance. The research highlighted the potential of affordable, 3D printed polymer-based materials in advancing the scalability and efficiency of MFC technology.

1.3 References of first chapter

[1] *Mashkour M., Rahimnejad M., Mashkour M., Soavi F., Electropolymerized polyaniline modified conductive bacterial cellulose anode for supercapacitive microbial fuel cells and studying the role of anodic biofilm in the capacitive behavior. J Power Sources* ***2020****, 478:1, 10*

[2] *Wilkinson S., ''Gastrobots'' – benefits and challenges of microbial fuel cells in food powered robot applications. Auton Robots* ***2000****, 9:99, 111*

[3] *Choudhury P., Ray R. N., Bandyopadhyay T. K., Tiwari O. N., Bhunia B., Kinetics and performance evaluation of microbial fuel cell supplied with dairy wastewater with simultaneous power generation. International Journal of Hydrogen Energy,* ***2021****, 46, 31, 16815-16822*

[4] *Mashkour M., Rahimnejad M., Mashkour M., Soavi F., Increasing bioelectricity generation in microbial fuel cells by a high-performance cellulose-based membrane electrode assembly. Appl Energy* ***2021****, 282:1, 11*

[5] *Yousefi V., Mohebbi-Kalhori D., Samimi A., Ceramic-based microbial fuel cells (MFCs): A review, International Journal of Hydrogen Energy* ***2017****, 42:3, 1672-1690*

[6] *Sanchez-Herrera D., Pacheco-Catalan D., Valdez-Ojeda R., Canto-Canche B., Dominguez-Benetton X., Domínguez-Maldonado J., Alzate-Gaviria L., Characterization of anode and anolyte community growth and the impact of impedance in a microbial fuel cell, BMC Biotechnology,* ***2014****, 14, 102*

[7] *Watanabe K. Recent developments in microbial fuel cell technologies for sustainable bioenergy, Journal of Bioscience and Bioengineering,* ***2008****, 106, 528–536*

[8] *Frijters C. T. M. J., Vos R. H., Scheffer G., Mulder R., Decolorizing and detoxifying textile wastewater, containing both soluble and insoluble dyes, in a full scale combined anaerobic/aerobic system, Water Research,* ***2006****, 40, 1249– 1257*

[9] *Malekmohammadi S., Mirbagheri S. A., A review of the operating parameters on the microbial fuel cell for wastewater treatment and electricity generation, Water Sci Technol,* ***2021****, 84, 6, 1309–1323*

[10] *R. H. Mahmoud, O. M. Gomaa, R.Y.A Hassan , Bio-electrochemical frameworks governing microbial fuel cell performance: technical bottlenecks and proposed solutions, RSC Advances,* ***2022***

[11] *M. Aghababaie, M. Farhadian, A. Jeihanipour, D. Biria, Effective factors on the performance of microbial fuel cells in wastewater treatment – a review, Environmental Technology Reviews,* ***2015****, 4, 1-19*

[12] *S. Gadkari, J.M. Fontmorin, E. Yu E, J. Sadhukhan, Influence of temperature and other system parameters on microbial fuel cell performance: Numerical and experimental investigation, Chemical Engineering Journal,* ***2020****, 388*

[13] *Nawaz A., Hafeez A., Abbas S. Z., Haq I., Mukhtar H., Rafatullah M., A state of the art review on electron transfer mechanisms, characteristics, applications and recent advancements in microbial fuel cells technology, Green Chemistry Letters and Reviews,* ***2020****, 13:4, 365-381*

[14] *Pandit S., Khilari S., Roy S., Pradhan, D., Das D., Bioresour. Technol.* ***2014****, 166, 451–457*

[15] *Malvankar N.S., Yalcin S.E., Tuominen M.T., Lovley D.R., Nat. Nanotechnol.* ***2014****, 9, 1012–1017*

[16] *Greenman J., Gajda I., You J., Mendis B. A., Obata O., Pasternak G., Ieropoulos I., Microbial fuel cells and their electrified biofilms, Biofilm, 3,* ***2021****, 100057*

[17] *Bayoudh S., Othmane A., Mora L., Ben Ouada H., Assessing bacterial adhesion using DLVO and XDLVO theories and the jet impingement technique, Colloids Surf B Biointerfaces,* ***2009****, 73, 1-9*

[18] *Chong P., Erable B., Bergel A., How bacteria use electric fields to reach surfaces, Biofilms****, 2021****, 3, 100048*

[19] *Brading M.G., Jass J., Lappin-Scott H.M., Dynamics of bacterial biofilm formation H.M. Lappin-Scott, J.W. Costerton (Eds.), Microb. Biofilms, Cambridge University Press,* ***2009****, 46-63*

[20] *Chung T.H., Dhar B.R., A MiniReview on Applications of 3D Printing for Microbial Electrochemical Technologies. Front. Energy Res.,* ***2021****, 9*

[21] *Kim, J., Kim, H., Kim, B., Yu, J., Computational Fluid Dynamics Analysis in Microbial Fuel Cells with Different Anode Configurations., Water Sci. Technol.* ***2014****, 69 (7), 1447–1452*

[22] *Massaglia, G., Gerosa, M., Agostino, V., Cingolani, A., Sacco, A., Saracco, G., et al. Fluid Dynamic Modeling for Microbial Fuel Cell Based Biosensor Optimization. Fuel Cells,* ***2017****, 17 (5), 627–634*

[23] *Yi Y., Xie B., Zhao T., Qian Z., Liu H., The Effect of Anode Hydrodynamics on the Sensitivity of Microbial Fuel Cell Based Biosensors and the Biological Mechanism. Bioelectrochemistry,* ***2020****, 132, 107351*

[24] *Parra-Cabrera, C., Achille, C., Kuhn, S., and Ameloot, R. 3D Printing in Chemical Engineering and Catalytic Technology: Structured Catalysts, Mixers and Reactors. Chem. Soc. Rev.,* ***2018****, 47 (1), 209–230*

[25] *Zhou Y., Tang L., Liu Z., Hou, J., Chen W., Li Y., et al. 2017 A Novel Anode Fabricated by Three-Dimensional Printing for Use in Urine-Powered Microbial Fuel Cell. Biochem. Eng. J.* ***2017****, 124, 36–43*

[26] *Calignano F., Tommasi T., Manfredi D., and Chiolerio A., Additive Manufacturing of a Microbial Fuel Cell—A Detailed Study. Scientific Rep.,* ***2015****, 5 (1), 1–10*

[27] *Pumera M., Three-dimensionally Printed Electrochemical Systems for Biomedical Analytical Applications. Curr. Opin. Electrochemistry* ***2019****, 14, 133–137*

[28] *Bian B., Shi D., Cai X., Hu M., Guo Q., Zhang C., et al., 3D Printed Porous Carbon Anode for Enhanced Power Generation in Microbial Fuel Cell. Nano Energy,* ***2018****, 44, 174–180*

[29] *He Y. T., Fu Q., Pang Y., Li Q., Li J., Zhu X., et al., Customizable Design Strategies for High-Performance Bioanodes in Bioelectrochemical Systems. Iscience,* ***2021****, 24 (3), 102163*

[30] *Zakaria B. S., Dhar B. R., Progress towards Catalyzing ElectroMethanogenesis in Anaerobic Digestion Process: Fundamentals, Process Optimization, Design and Scale-Up Considerations. Bioresour. Technol.* ***2019****, 289, 121738*

[31] *Freyman M. C., Kou T., Wang S., Li Y. 2020 3D Printing of Living Bacteria Electrode. Nano Res.,* ***2020****, 13 (5), 1318–1323*

[32] *Qian F., Zhu C., Knipe J. M., Ruelas S., Stolaroff J. K., DeOtte J. R., et al., Direct Writing of Tunable Living Inks for Bioprocess Intensification. Nano Lett.,* ***2019****, 19 (9), 5829–5835*

[33] *Asthana M., Kumar A., Sharma B. S., Principles and Applications of Environmental Biotechnology for a Sustainable Future,* ***2017****, 173-232*

[34] *Gašpariková E., Kapusta S., Bodík I., Derco J., Kratochvíl K., Evaluation of Anaerobic-Aerobic Wastewater Treatment Plant Operation. Polish Journal of Environmental Studies,* ***2005****, 14, 29-34*

[35] *Sawyer C. N., McCarty P. L., Parkin G. F., Chemistry for Environmental Engineering and Science (5th ed.),* ***2003****, New York: McGraw-Hill*

[36] *N. Kularatna, K. Gunawardane, Fundamentals of energy storage devices, Energy Storage Devices for Renewable Energy-Based Systems (Second Edition), Academic Press,* ***2021****, 37-64*

2. Materials and methods

2.1 Materials

2.1.1 Acrylonitrile Butadiene Styrene (ABS) - Carbon Composite

ABS is a polymer obtained by copolymerization of three monomers of acrylonitrile (A, 23%–41%), butadiene (B, 10%–30%), and styrene (*S*, 29%–60%). ABS is produced by emulsion or continuous mass technique. The chemical formula of Acrylonitrile Butadiene Styrene is $(C_8H_8 \cdot C_4H_6 \cdot C_3H_3N)_n$. The natural material is an opaque ivory color. It is readily colored with pigments or dyes. The macromolecular main chain of ABS is repeatedly connected by three structural units. Different structural units give ABS different properties: acrylonitrile has good chemical resistance and high surface hardness; butadiene has good toughness; and styrene has good transparency and processing performance. When the three monomers are combined, the tough, hard, and rigid ABS resin is formed. [1] [2] [3]

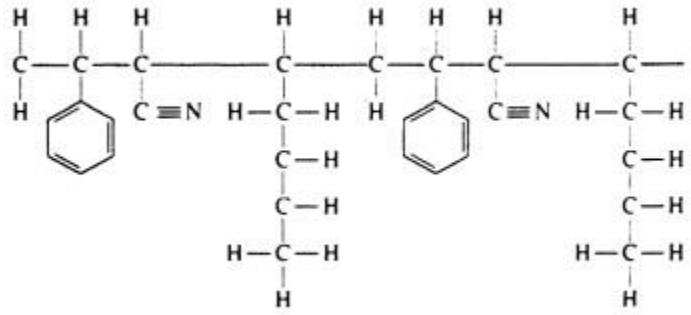

Figure 5: *Molecular Structure of Acrylonitrile Butadiene Styrene*

The heat distortion temperature of ABS is 93°C–118°C. ABS can be used in a temperature range of −40°C–100°C. The specific properties are shown in Table 1.

Relative density	**Water absorption rate (%)**	**Molding shrinkage (%)**	**Tensile strength (MPa)**	**Bending strength (MPa)**	**Rockwell hardness**	**Heat distortion temperature (°C)**	**Linear expansion coefficient ($\times 10^{-5} K^{-1}$)**
1.02–1.05	0.2–0.45	0.3–0.8	35–44	51–81	R65–109	93–103	9.5–10.5

Table 1: *Properties of ABS materials [1]*

In this work, we utilized an ABS-carbon fiber composite by 3DXTECH for the anodes and cathodes. The integration of carbon fibers into the ABS matrix not only provided the desired mechanical properties, but also ensured the material's electrical conductivity, which was crucial for the purpose of this work.

Carbon fiber reinforced filaments, specifically those integrated with ABS (Acrylonitrile Butadiene Styrene), consist of fibers that are 5-10 micrometers wide made of carbon. These fibers are meticulously aligned along the axis of the material, a feature that, combined with their inherent physical properties, imparts exceptional characteristics to the composite. Carbon fibers are renowned for their high stiffness, high tensile strength, excellent heat tolerance, high chemical resistance, low weight, and minimal thermal expansion. By reinforcing ABS plastic with carbon fibers, a 3D printing filament is produced that showcases the advantageous properties of both components. This combination results in a material that is both lightweight and rigid, making it ideal for applications that demand these qualities. Consequently, carbon fiber reinforced parts are extensively utilized in fields such as aerospace, civil engineering, military, and motorsports, where reducing material usage and saving weight are critical considerations.

In order to 3D print the ABS-CF composite in the intricate designs that were needed for the experiment, the 3D modeling program Tinkercad was used. The designs of both the anode and the cathodes, as well as the final 3D printed material are shown in Figures 6-9 below. The dimensions of the cathodes are 6 cm by 6 cm, while the anode measures 4.5 cm by 4.5 cm by 4.5 cm.

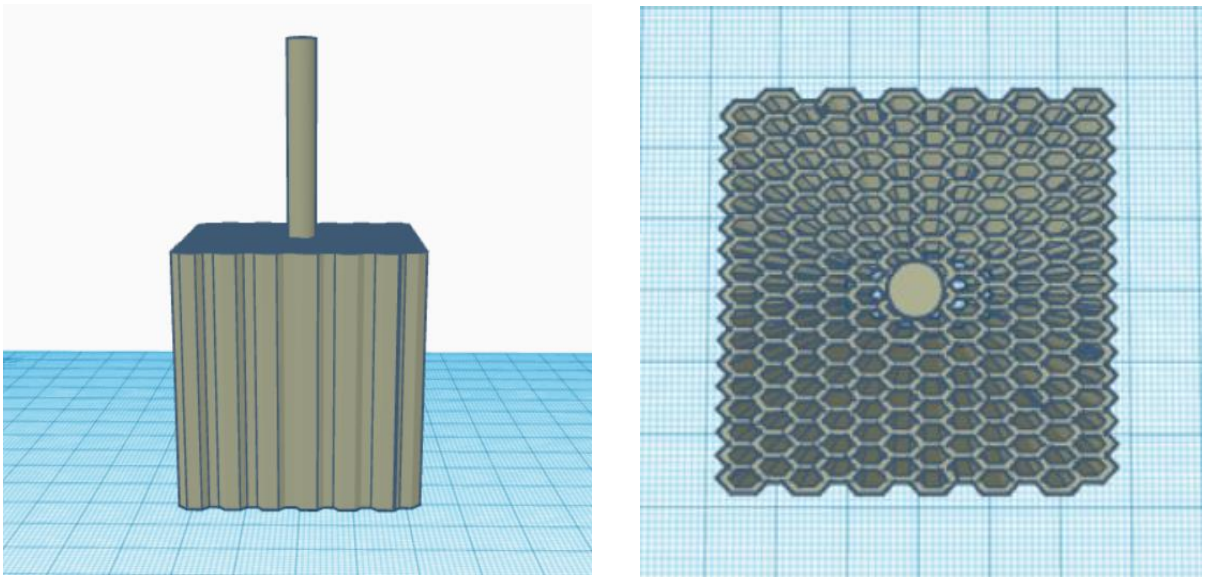

Figure 6: *Design of the anode*

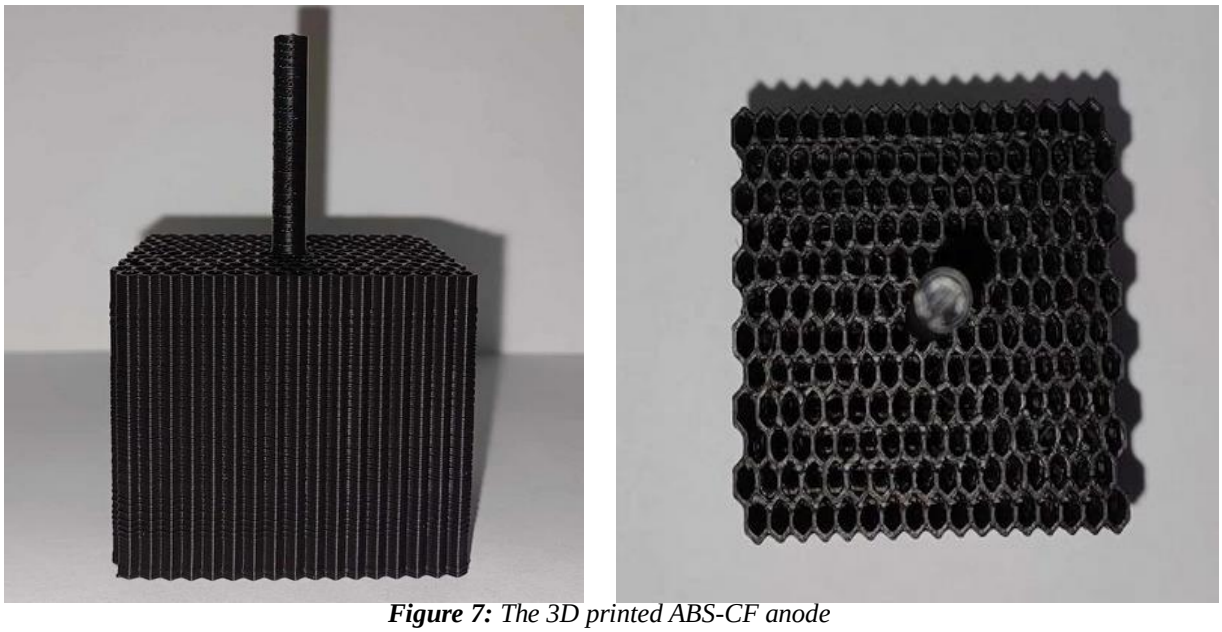

Figure 7: *The 3D printed ABS-CF anode*

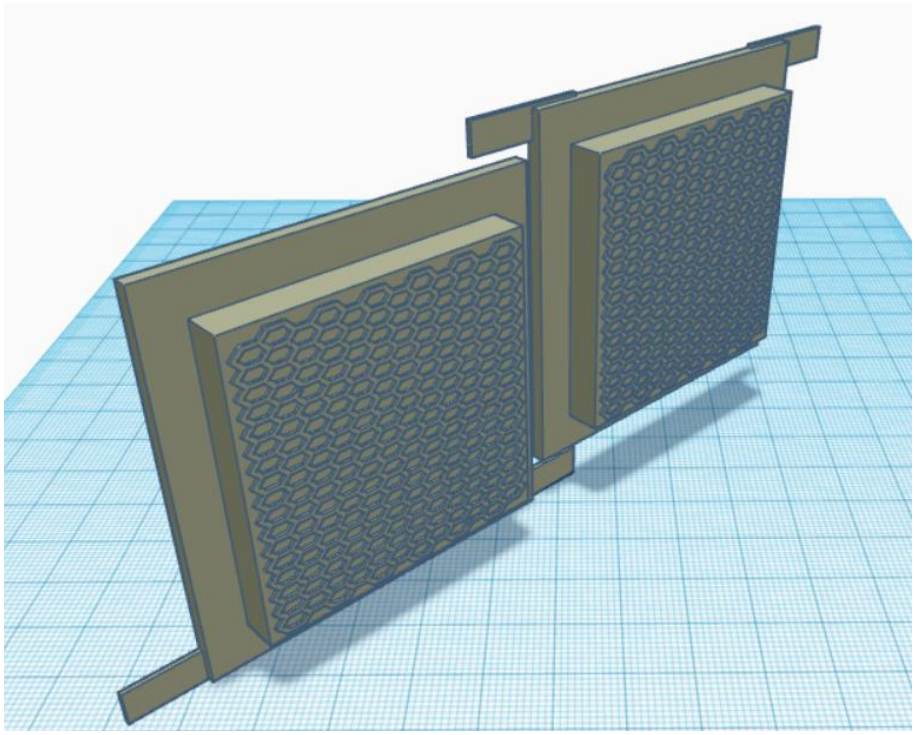

Figure 8: *Design of the cathodes*

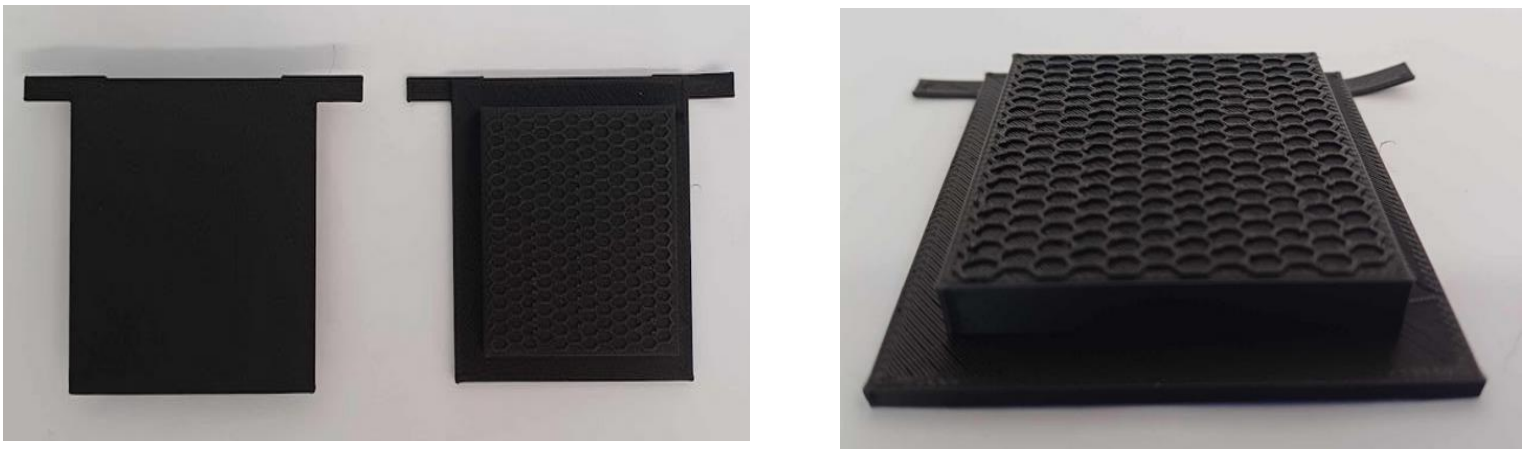

Figure 9: *The 3D printed ABS-CF cathodes*

The intricate geometry of the anode and the air cathodes was deliberately selected to maximize the surface area, which is crucial for enhancing microbial activity. The increased surface area of the electrodes significantly contributes to the better performance of the MFCs. [4]

2.1.2 Assembly of MFCs

Based on the evaluation of previous research findings, we determined the following to be the final structure of the MFC. [5][6][7][8][9][10][11][12] The air-cathode, membrane-less single-chamber Microbial Fuel Cells (MFCs) were crafted from Plexiglas, boasting a total volume of 448 ml and built in a cubic form. The anode was placed within this chamber and fixed to the upper surface of the cells, while the air cathodes were positioned along the four vertical sides, all interconnected with wires. The assembly process involved initially welding the Plexiglas sides using chloroform, followed by reinforcing the bonds with a heat gun for enhanced structural integrity. To complete the construction, inlet and outlet openings were installed on the top and bottom sides of the cells, respectively.

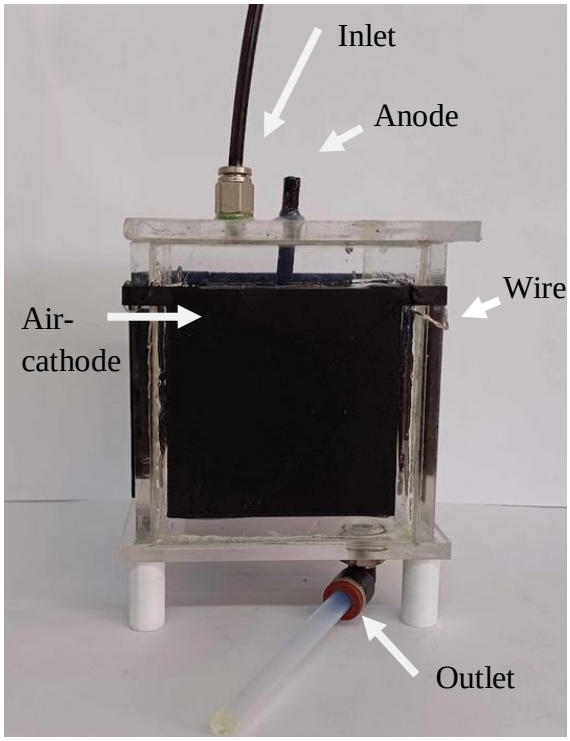

***Figure 8**: Experimental configuration of the single-chamber MFC*

2.1.3 Anodic electrolyte solution

The anolyte solution that was used for the inoculation process, consisted of the following components:

- 275ml buffer solution
- 36,5ml glucose solution
- 9,1ml of inoculum with E. coli bacteria, which were grown in Luria - Bertani (LB) medium, at 37^{o}C, at 180 rpm, for 24 hours. The growth of the bacterium was monitored by measuring the optical density at 600 nm.
- 20ml KCl
- 36,5ml of electrolyte solution that consisted of Na_2CO_3, $NaHCO_3$ and $K_4P_2O_7$

After the inoculation, the anodic electrolyte solution that was used for each of the operating cycles of the MFC consisted of

- 275ml buffer solution
- 36,5ml glucose solution
- 20ml KCl
- 36,5ml of electrolyte solution that consisted of Na_2CO_3, $NaHCO_3$ and $K_4P_2O_7$

2.2 Experimental Techniques

As microbial fuel cells are devices that produce power, their electrochemical characterization is considered to be of key importance. Several techniques are used for the understanding of their operation and the individual internal parameters that make the cells functional and efficient. These techniques are non-destructive and provide a clear insight into the electrochemical behavior of the materials used to compose the final electrode and the electrode-electrolyte relationship.

Throughout the duration of the present work the experimental techniques used were

- Open Current Voltage OCV
- Cyclic Voltammetry CV
- I-V Characterization IVC
- Potentiostatic Electrochemical Impedance Spectroscopy PEIS

For all the above experimental techniques performed the SP-150 potentiostat/ galvanostat was used, which was controlled with EC-Lab software.

Except for the techniques mentioned above, COD measurements also took place, as well as pH and conductivity measurements of the anolyte solutions. The quality of the MnO_2 coatings was determined by scanning electron microscopy (SEM).

2.3 References of second chapter

[1] *Shi Y., Zhou Y., Wang Y., Chen Y., Yan C., Wu J., Yu S., Materials for additive manufacturing,* ***2021***

[2] *Plastic Properties of Acrylonitrile Butadiene Styrene (ABS), the Wayback Machine,* ***2010***

[3] *S. Vishwakarma, Characterization of ABS Material: A Review, Quest Journals,*

2017

[4] *C. Picioreanu, M.C.M. van Loosdrecht, T. P. Curtis, K. Scott, Model based evaluation of the effect of pH and electrode geometry on microbial fuel cell performance, Bioelectrochemistry,78, 1,* ***2010***

[5] *A. Tremouli, P. K. Pandis, T. Kamperidis, C. Argirusis, V.N. Stathopoulos, G. Lyberatos, Performance comparison of different cathode strategies on air-cathode microbial fuel cells: Coal fly ash as a cathode catalyst. Water* ***2023****, 15, 10*

[6] *Pandis, P.K., Michopoulos E., Arvanitis, C., Argirusis C., Stathopoulos V.N., Lyberatos G., Tremouli A., Bioenergy production from tannery waste via a single-chamber microbial fuel cell with fly ash cathodic electrodes. Key Engineering Materials* ***2023****, 962, 105-112*

[7] *Pandis P.K., Georgala M., Nanou P., Stathopoulos V.N., Fabrication and study of 3d printed abs-carbon composite anodes for single chamber microbial fuel cells. Key Engineering Materials* ***2023****, 962, 113-120*

[8] *Savvidou M.G. Pandis P.K. Mamma D. Sourkouni G. Argirusis C., Organic waste substrates for bioenergy production via microbial fuel cells: A key point review. Energies* ***2022****, 15, 5616*

[9] *Kamperidis T., Pandis P.K., Argirusis C., Lyberatos G., Tremouli A., Effect of food waste condensate concentration on the performance of microbial fuel cells with different cathode assemblies. Sustainability* ***2022****, 14, 2625*

[10] *Tremouli A., Pandis P.K., Karydogiannis I., Stathopoulos V.N., Argirusis C., Lyberatos G., Operation and electro(chemical) characterization of a microbial fuel cell stack fed with fermentable household waste extract. Global NEST Journal* ***2019****, 21, 253-257*

[11] *Tremouli A., Pandis P.K., Kamperidis T., Stathopoulos V.N., Argirusis C., Lyberatos G., Performance assessment of a four-aircathode membraneless microbial fuel cell stack for waste water treatment and energy extraction. E3S Web of Conferences* ***2019****, 116, 00093*

[12] *Tremouli A., Karydogiannis I., Pandis P.K., Papadopoulou K., Argirusis C., Stathopoulos V.N., Lyberatos G., Bioelectricity production from fermentable household waste extractusing a single chamber microbial fuel cell. Energy Procedia* ***2019****, 161, 2-9*

3. Results and discussion

3.1 Chemical modification of electrodes

While the ABS-carbon composite inherently possesses electrical conductivity, it must be further modified to be conducive to microbial activity. This modification is essential for facilitating the formation of a biofilm on the anode in microbial fuel cells (MFCs). The treatment process should enhance the surface properties of the composite to support microbial adhesion and growth, thereby optimizing the biofilm formation necessary for efficient electron transfer. Without this crucial step, the composite, despite its conductivity, would not effectively support the microbial processes integral to the operation of MFCs.

To address these requirements, two treatments were selected: chemical modification using acetone and chemical modification using NaOH.

3.1.1 Chemical modification of electrodes with acetone

In order to enhance the surface properties of ABS, it was initially treated with acetone. This processing step was undertaken for several reasons:

1. Surface Activation: Acetone treatment can modify the surface characteristics of ABS-CF, making it more conducive to further chemical treatments or coatings. Brief exposure to acetone can cause slight surface swelling and softening, potentially increasing the surface area and improving the adherence of subsequent chemical compounds or microbial biofilms, which are critical for the efficiency of the microbial fuel cells.
2. Cleaning and Degreasing: Acetone is an effective solvent for removing surface contaminants such as oils, greases, and residues that may be present on the ABS material from the manufacturing process. A clean surface is essential for ensuring consistent and reliable electrochemical measurements in MFCs. By briefly immersing the ABS-C in acetone, we ensured that the surface was free from contaminants that could interfere with the electrochemical performance.
3. Surface Smoothing: Exposure to acetone can smooth the surface of ABS-CF by dissolving the outermost layer of the polymer. This smoothing effect can be beneficial in creating a uniform and clean surface, which can help in achieving more consistent electrochemical interactions and measurements. The smoother surface can also reduce the presence of micro-defects that might act as sites for unwanted reactions or variability in the electrochemical performance.

Sample preparation method

In order to be able to determine the most effective way of properly processing the ABS-C before installing it on the MFCs, a series of tests were performed. For the purpose of the following tests, used 3D printed ABS-CF samples of three different dimensions 7,85cm^2 19.16 cm^2 and 14,545cm^2 were used.

The samples were immersed in acetone for 20 seconds, after that they were rinsed with distilled water and left to dry for either 10 minutes, one day or three days. Differences in the CV curves were noticed, based on the time of drying.

Sample name	Sample dimensions(cm^2)	Drying time(h)
BLANK	7.85	-
AC 1	7.85	0.17
AC 2	19.16	0.17
AC 3	7.85	24
AC 4	19.16	24
AC 5	7.85	72
AC 6	14.545	72

Table 2: *The characteristics of the samples used*

Experimental Method

0,1 M $KMnO_4$ solution (1,26g $KMnO_4$ in 79ml H_2O) was used for all the electrochemical tests.

For all three experimental techniques performed the SP-150 potentiostat/ galvanostat was used, which is controlled with EC-Lab software. The reference electrode was a saturated Ag/AgCl electrode, for the counter electrode we used a thin sheet of stainless steel 304, lastly the working electrode was the ABS-CF sample.

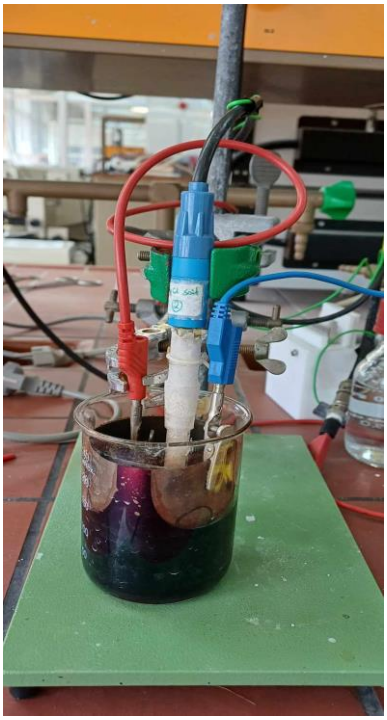

Figure 9: *Experimental setup used for OCV, CV and Mn deposition*

An open-circuit voltage (OCV) measurement was conducted to assess the electrochemical stability of the samples. The potential of the working electrode (E_{we}) ranged from 1,5 to 0,55 V over the 20 minutes the measurement run. This fluctuation could indicate that the ABS-C surface did not remain chemically inert, showing signs of degradation or redox activity.

After the OCV measurements, we run in the same $KMnO_4$ solution, a cyclic voltammetry measurement (CV) for each sample to evaluate the electrochemical properties. The range of potential for the CV measurements was -3 - 3 V and the duration was 1 hour and 20 minutes.

As shown in Figure 10, it was observed that the current (I) varied significantly depending on the drying time of the samples post-acetone treatment. This variation can be attributed to the fact that as the acetone evaporates, the polymer chains in ABS may partially recover their original structure. The extent and uniformity of this reformation process depend on the drying duration, impacting the electrochemical properties of the surface. Adequate drying time ensures that the surface properties of ABS-CF stabilize, resulting in more consistent and reliable electrochemical measurements.

CV Diagrams

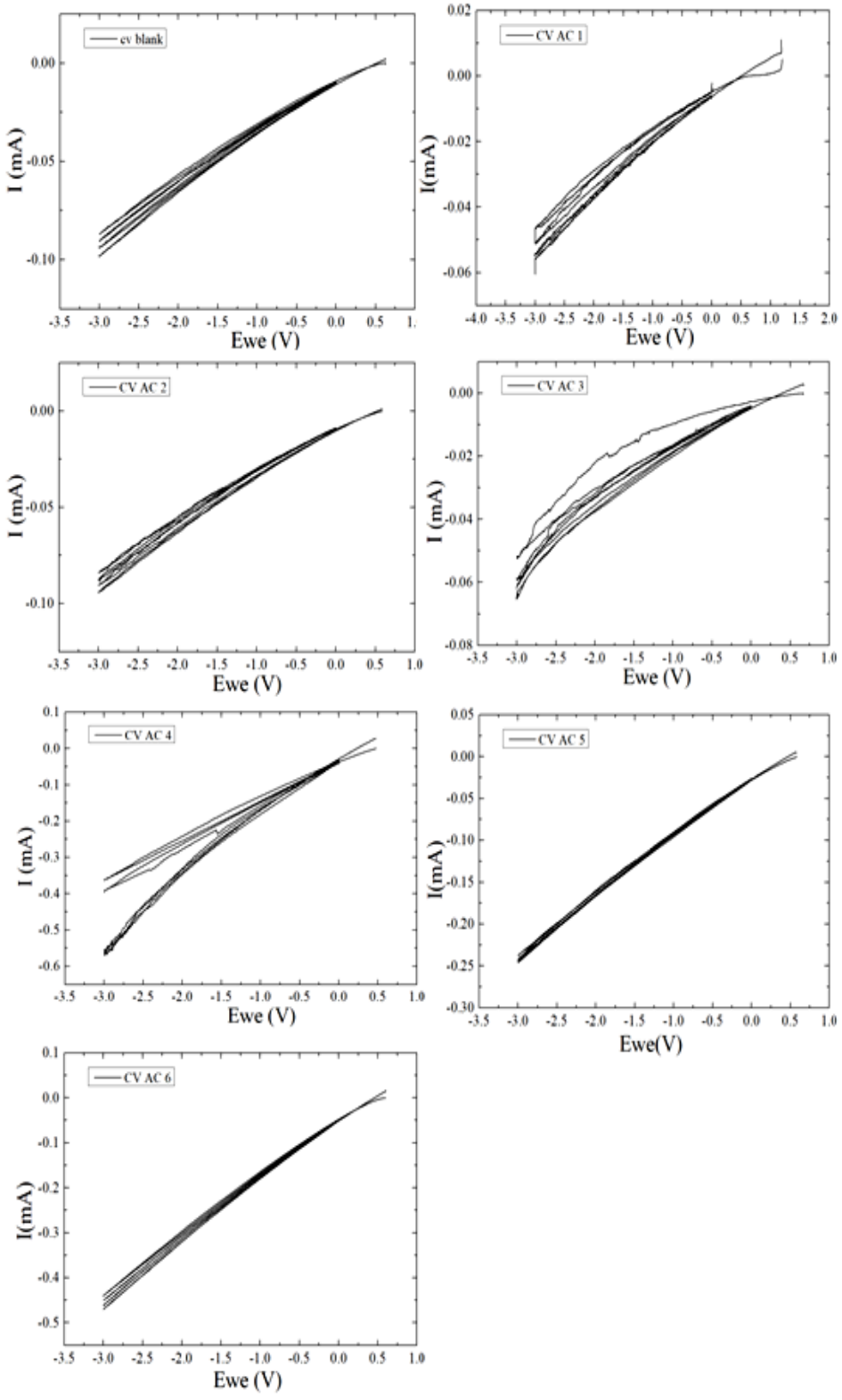
cv blank
I (mA)
Ewe (V)
CV AC 1
I(mA)
Ewe (V)
CV AC 2
I (mA)
Ewe (V)
CV AC 3
I (mA)
Ewe (V)
CV AC 4
I (mA)
Ewe (V)
CV AC 5
I(mA)
Ewe(V)
CV AC 6
I(mA)
Ewe (V)

Figure 10: *CV curves of ABS-C samples after the chemical processing with acetone*

Manganese dioxide deposition

After conducting OCV and CV measurements, electrochemical deposition of manganese dioxide (MnO_2) was performed on the samples. The current applied during the deposition process corresponded to the midpoint of the current observed in the CV curve for each sample. This approach ensured that the deposition conditions were tailored to the specific electrochemical characteristics of each individual sample, promoting the most consistent and optimal formation possible of the MnO_2 layer. The duration of all depositions was four hours.

The mass of each sample was measured before the preparation (**m_1**), right after the immersion in acetone (**m_2**), after the drying (**m_3**) and after the deposition (**m_4**).

Sample name	m_1(g)	m_2(g)	m_3(g)	m_4(g)
BLANK	0.4722	-	-	-
AC 1	0.4818	0.4850	0.4850	0.4832
AC 2	1.3183	1.3232	1.3232	1.3191
AC 3	0.4690	0.4721	0.4684	0.4697
AC 4	1.0737	1.0824	1.0733	1.0744
AC 5	0.4754	0.5604	0.4735	0.4767
AC 6	0.9921	1.0781	0.9925	0.9940

Table 3: *The masses of the samples throughout the experimental process*

Sample name	% Increase of mass
AC 1	0.3
AC 2	0.06
AC 3	0.14
AC 4	0.07
AC 5	0.3
AC 6	0.2

Table 4: *The percentage of mass increase after the MnO_2 deposition*

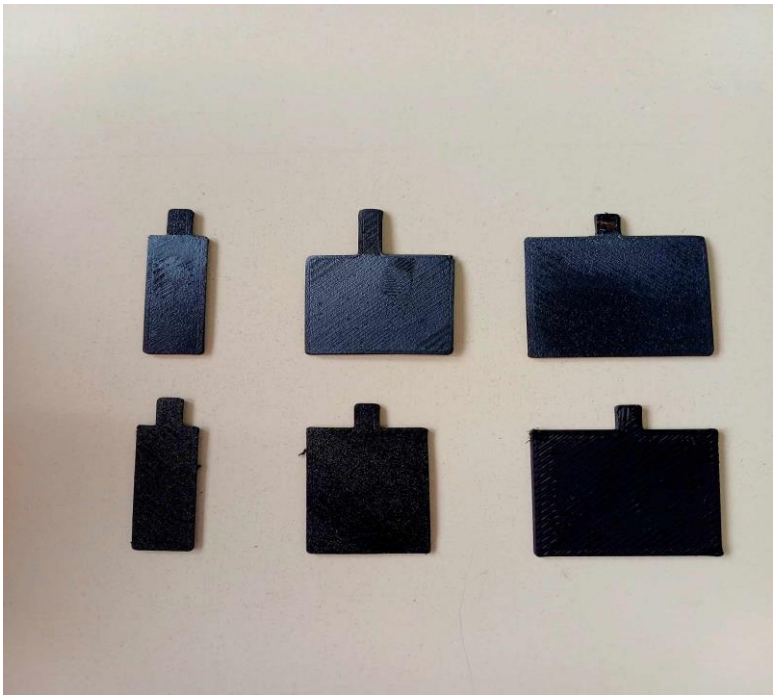

Figure 11: *Samples before (down) and after (up) the MnO_2 deposition*

Following the MnO_2 deposition, it was noted that the mass increase, as shown in Table 3 was not proportional to the surface area of the samples. This disproportionate mass increase can be explained by several factors, including non-uniform deposition due to variations in surface properties and local current densities, differences in surface roughness and morphology, and variations in current distribution during the deposition process. Furthermore, the applied current, based on the midpoint of the CV curve, may not have perfectly accounted for the differences in surface areas leading to less efficient deposition on some samples. Additionally, the actual accessible surface area for MnO_2 deposition might differ from the geometric surface area due to surface irregularities, resulting in varying amounts of MnO_2 being deposited.

3.1.2 Chemical modification of electrodes with NaOH

After the acetone processing, it was determined that it would be beneficial to explore an alternative treatment method using sodium hydroxide (NaOH) for processing the ABS-CF samples. This decision was made to investigate the potential improvements in surface preparation and electrochemical performance that NaOH treatment might offer compared to acetone. The NaOH treatment is known to denitrogenate ABS, which can offer several benefits, particularly in the context of improving the material's surface properties and enhancing electrochemical performance in the MFCs. [2]

1. Surface Activation and Functionalization: The NaOH treatment could potentially introduce oxygen-containing functional groups, such as hydroxyl and carboxyl groups on the ABS surface. This functionalization increases the number of reactive sites available for subsequent chemical reactions or microbial biofilm attachment, enhancing the interaction between the ABS and the electrolyte.
2. Enhanced Electrochemical Performance: By removing nitrogen-based impurities, NaOH treatment helps purify the material's surface, leading to more stable and reproducible electrochemical measurements. The functionalized surface also improves the adherence and uniformity of electrodeposits, such as MnO_2, by providing a more chemically active surface.
3. Structural and Mechanical Stability: NaOH treatment can etch the material's surface, creating a rougher texture that enhances the mechanical interlocking between the ABS-CF substrate and the electrodeposited layers. This modification can improve the structural integrity and durability of the composite material used in MFC components.
4. Enhanced Microbial Adhesion: The increased hydrophilicity and surface roughness resulting from NaOH treatment promotes better microbial adhesion and biofilm formation, which are essential for the efficient operation of MFCs.

Sample preparation method

For this set of tests, all three samples used had uniform dimensions of 6x6 cm. This specific shape was chosen because it closely resembles the shape of the cathodes that would eventually undergo the same modifications and MnO_2 deposition processes. This consistency in sample dimensions ensured that the results were directly applicable to the final cathode design, allowing for more accurate and relevant comparisons of the electrochemical performance and material properties after each treatment step.

The samples were immersed in a 3M NaOH solution for 30 minutes. Following immersion, the samples were thoroughly rinsed with distilled water to remove any residual NaOH. The rinsed samples were then left to dry for 24 hours.

Experimental Method

0,1 M $KMnO_4$ solution (3.16g $KMnO_4$ in 198ml H_2O) was used for all the electrochemical tests.

For all three experimental techniques performed OCV, CV, and MnO_2 deposition the same SP-150 potentiostat/galvanostat was utilized, as in the acetone modification. The reference electrode employed was a saturated Ag/AgCl electrode, while a stainless steel 304 plate served as the counter electrode. The ABS-CF samples functioned as the working electrodes.

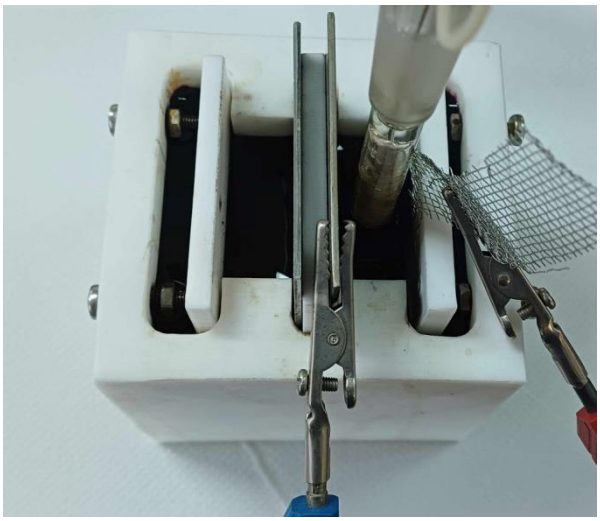

Figure 12: *Experimental setup used for OCV, CV and MnO_2 deposition*

OCV measurement was again conducted to assess the electrochemical stability of ABS-CF. The potential of the working electrode (E_{we}) remained almost stable at 0,6V over the 20 minutes the measurement run. The stable potential indicated that the ABS surface remained chemically inert and stable in the electrolyte, showing no signs of degradation or redox activity. This stability suggested that the NaOH treatment effectively prepared the surface by removing contaminants, making it clean and suitable for use in the microbial fuel cell. Additionally, the non-reactive interaction between the ABS and the electrolyte confirmed the material's compatibility and suitability for structural components within MFCs, ensuring reliable performance in the electrochemical environment. After the OCV measurements, a CV measurement was run in the same $KMnO_4$ solution for each sample to evaluate the electrochemical

properties. The range of potential for the CV measurements was -3 - 3 V and the duration was 1 hour and 20 minutes.

CV Diagrams

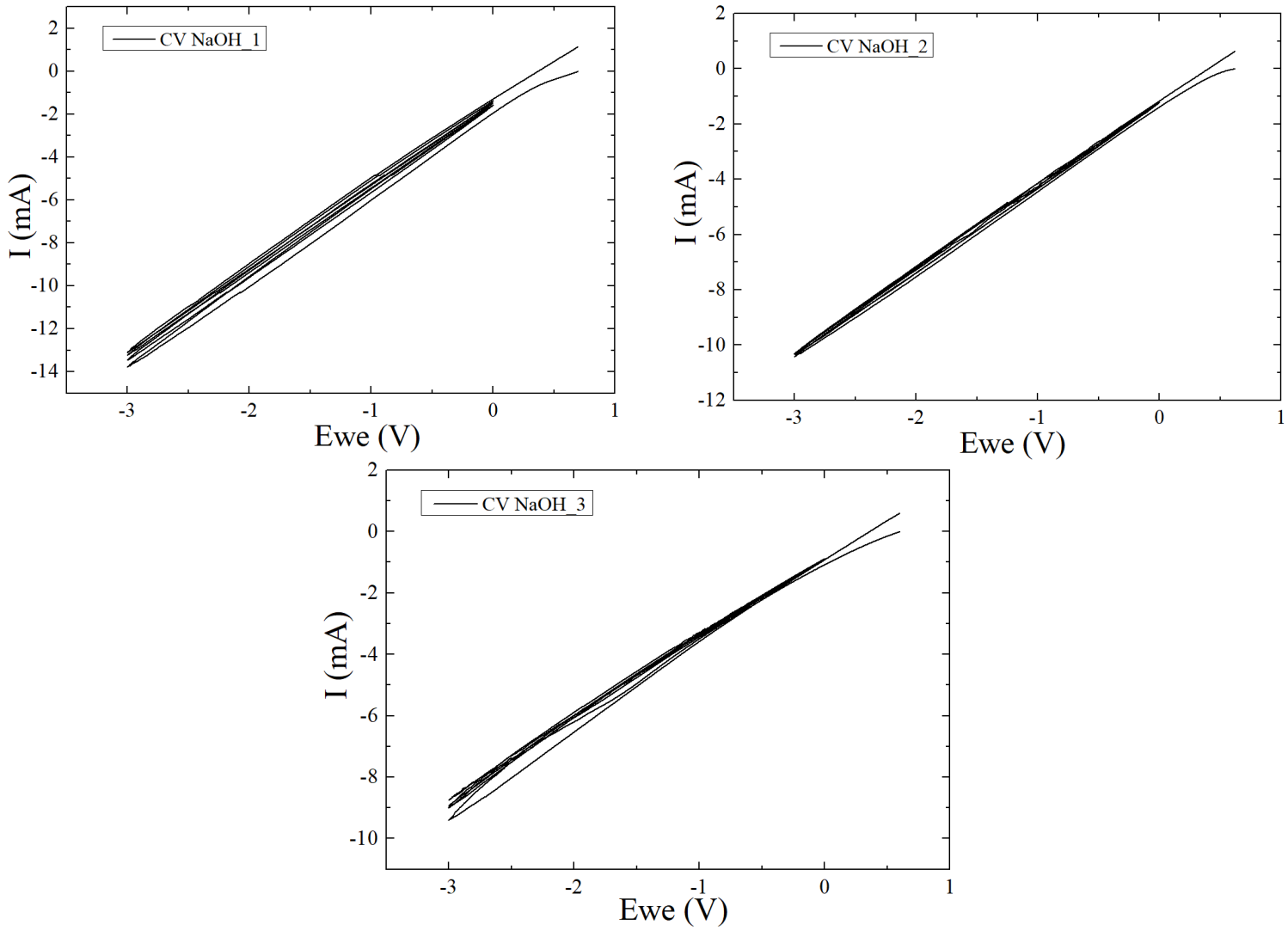

Figure 13: *CV curves of ABS samples after the chemical processing with NaOH*

Manganese dioxide deposition

After conducting OCV and CV measurements, electrochemical deposition of manganese dioxide (MnO_2) was performed on the ABS-CF samples. The current applied during the deposition process was -5mA, this corresponded to the midpoint of the current observed in the CV curve. The duration of the depositions was four hours.

The mass of each sample was measured before the preparation ($\mathbf{m_1}$), after the drying ($\mathbf{m_2}$) and after the deposition ($\mathbf{m_3}$).

Sample name	m_1(g)	m_2(g)	m_3(g)
NaOH_1	4.8013	4.6486	4.7134
NaOH_2	4.7931	4.6345	4.7026
NaOH_3	4.7986	4.6387	4.7027

Table 5: *The masses of the samples throughout the experimental process*

Sample name	% Increase of mass
NaOH_1	1.39
NaOH_2	1.46
NaOH_3	1.38

Table 6: *The percentage of mass increase after the MnO_2 deposition*

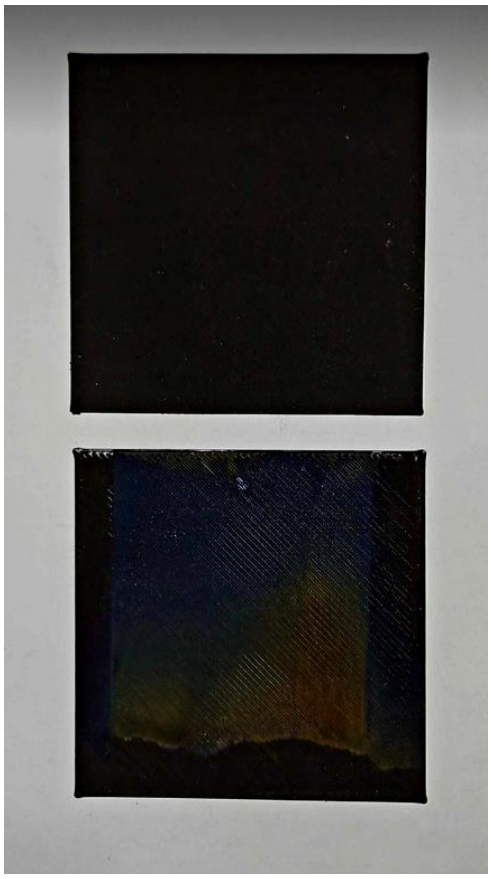

Figure 14: *Samples before and after the MnO_2 deposition*

The increase in mass observed in all three samples after the MnO_2 deposition was notably consistent. This consistency, as well as the consistency of the OCV measurements and CV diagrams, provided us with the evidence needed for proceeding with the NaOH processing for the actual electrodes used in the MFCs.

3.2 Optical characterisation of the MnO_2 coatings

After conducting the modifications and the depositions mentioned above, we aimed to evaluate the quality and uniformity of the MnO_2 coatings on the ABS samples. This analysis was performed using scanning electron microscopy (SEM), which provided detailed images of the surface morphology and distribution of the MnO_2 layers, allowing us to assess the effectiveness of the deposition process. For these test the TM3030Plus Tabletop Microscope by Hitachi was used. The samples tested included one that was treated with acetone and left to dry for 72 hours before MnO_2 deposition (Acetone-MnO_2), one that was treated with NaOH followed by MnO_2 coating (NaOH-MnO_2), and one that was treated with NaOH without the MnO_2 coating (NaOH).

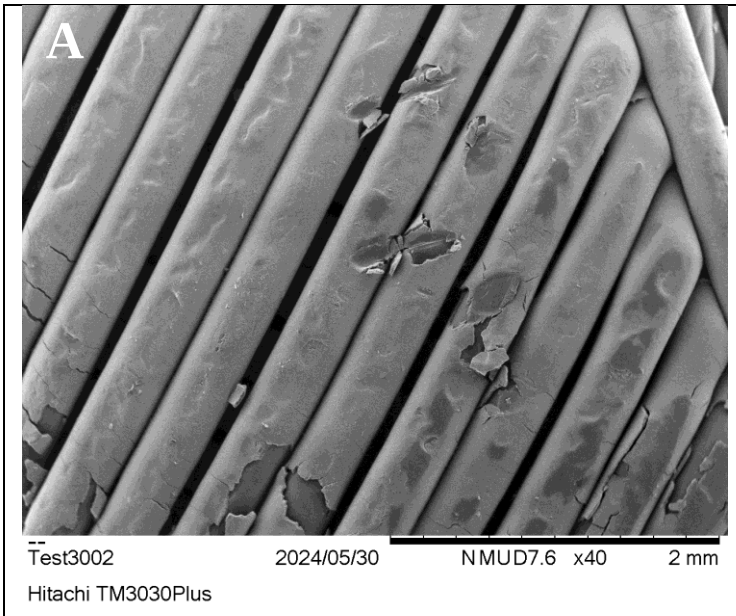

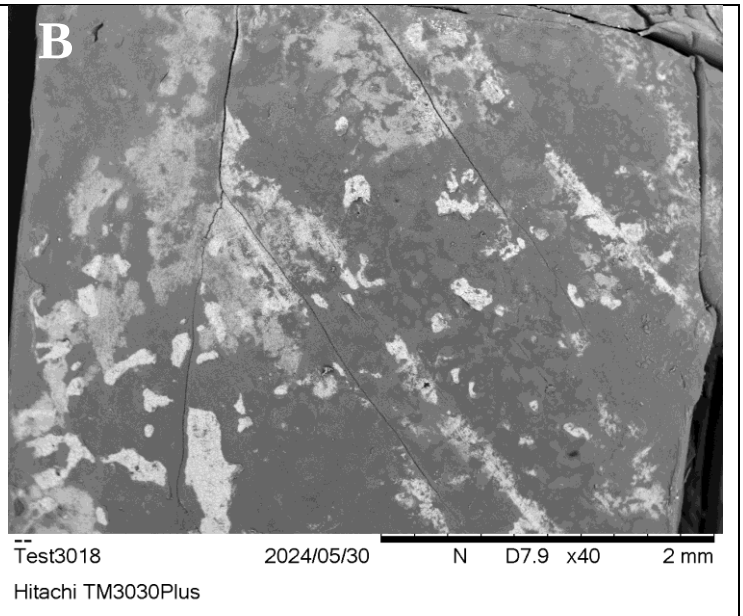

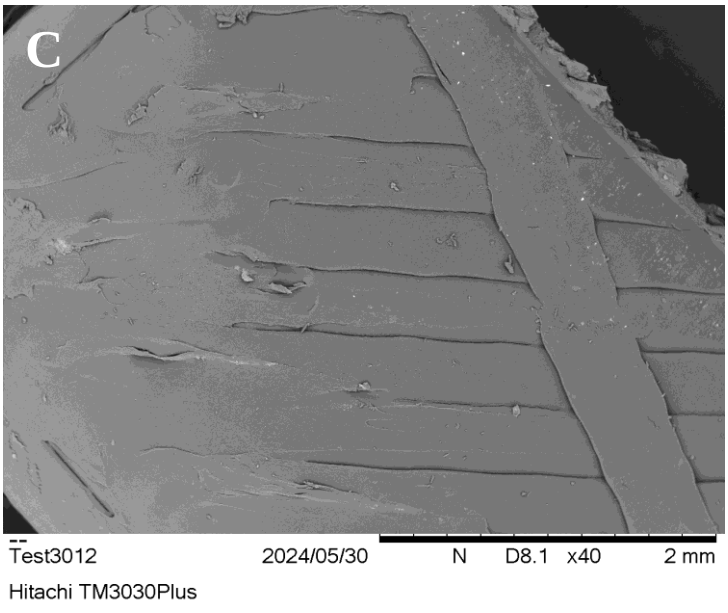

Figure 15: *SEM images of A) sample NaOH-MnO_2, B) sample Acetone-MnO_2, C) sample NaOH*

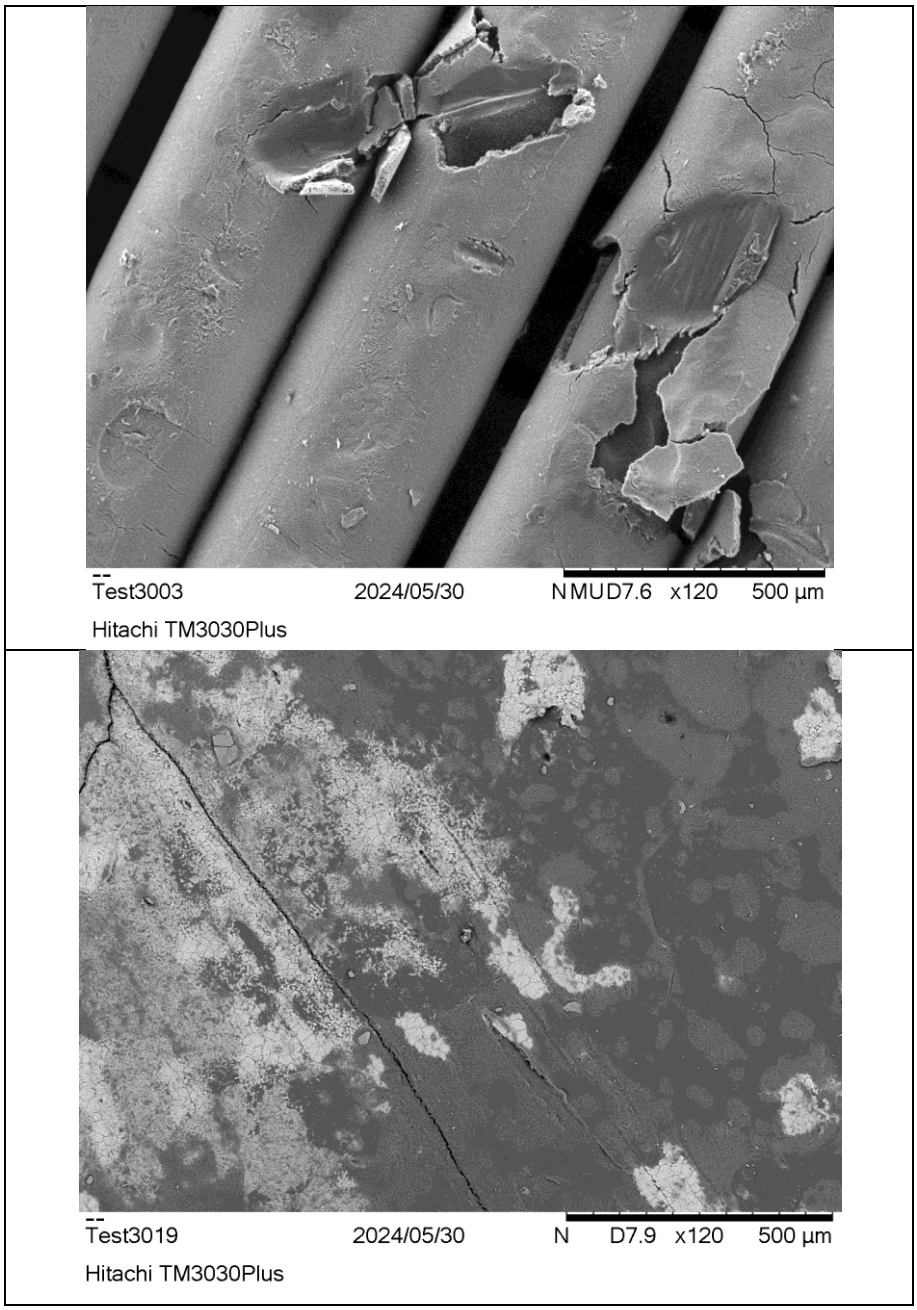

Figure 16: *SEM images of sample NaOH-MnO_2 (up) and ABS sample Acetone-MnO_2 (down)*

In Figure 16, we observe the two MnO_2-coated samples at higher magnification. Prior to imaging, the coatings were intentionally slightly damaged to facilitate measurement of the coating thickness. The left image shows the MnO_2-NaOH sample, which exhibits a uniform MnO_2 layer. On the other hand, the right image of the acetone-MnO_2 sample reveals areas that remain uncoated (indicated by the darker regions), indicating inconsistencies in the coating application.

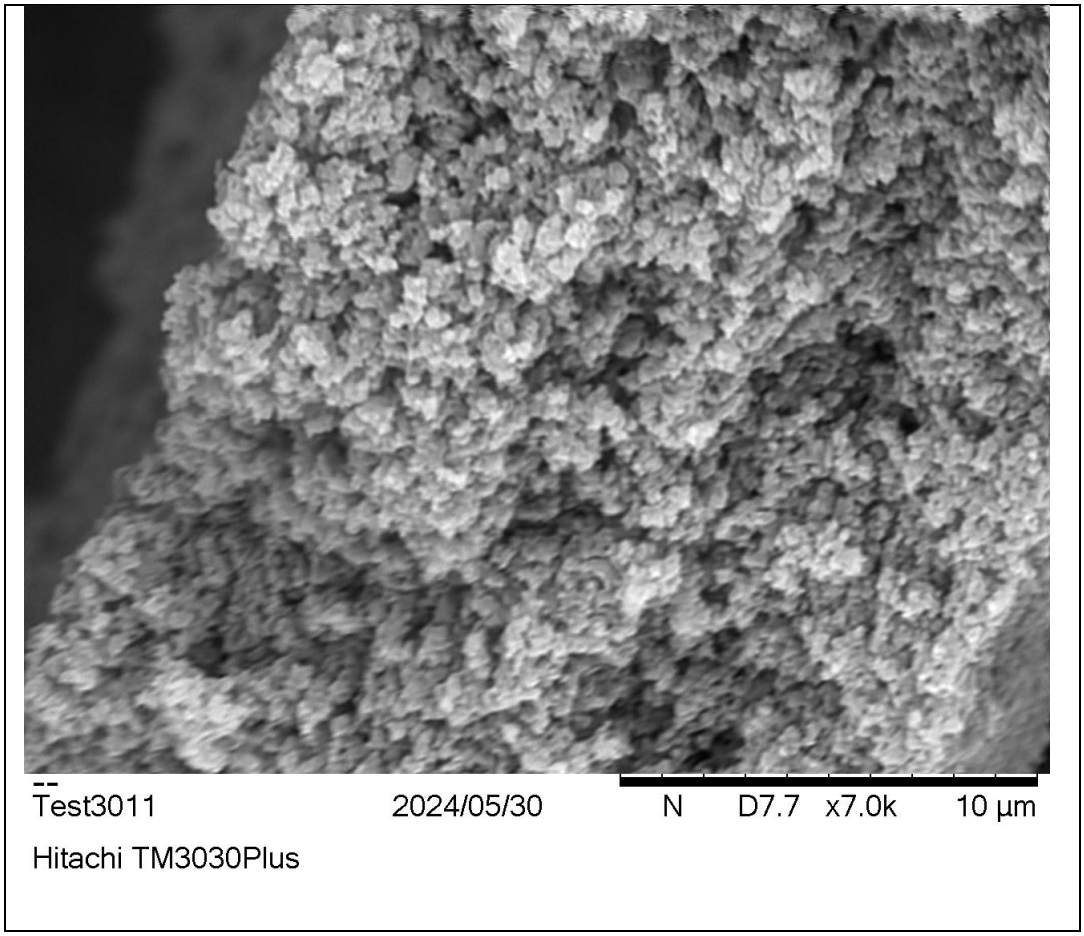

Figure 17: *SEM images of sample NaOH-MnO_2*

In Figure 17, it is evident that the MnO_2 layer on the MnO_2-NaOH sample has a thickness of approximately **20 µm**. The thickness and uniformity of the MnO_2 coating observed in this sample were the primary reasons for choosing the NaOH treatment for the actual electrodes used in the cell.

3.3 Manganese dioxide deposition of the cathode electrodes

Following the preliminary tests, we proceeded with the NaOH processing of both the anode and cathodes for the two MFCs constructed for this thesis. In one of the two cells, both the anode and cathodes underwent NaOH treatment. In the second cell, the cathodes were not only treated with NaOH, but also coated with MnO_2. This dual approach was intended to compare the effects of NaOH treatment alone against the combined treatment of NaOH and MnO_2 coating on the electrochemical performance and efficiency of the MFCs.

In recent years, non-precious metals have been tested as potential options for ORR catalysts in MFCs. Platinum group metal-free (PGM-free) catalysts are a class of catalysts that include transition metals (Fe, M, Mn, Cu) and carbon-based materials with heteroatom admixture. Most of these catalysts have demonstrated excellent electrocatalytic activity. [3]

Transition metal oxides (TMOs) are a broad family of electrocatalysts that constitute of monoxides and mixed metal oxides. Compared to catalysts based on Pt, TMO-based catalysts have many advantages, such as being economical and more abundant,easy to synthesize and environmental friendly. TMOs acquire multiple valence states, allowing them to have various electrocatalytic applications. [4]

Manganese oxides can function simultaneously as an ORR and OER catalyst, thus making it an interesting bifunctional catalyst for oxygen electrochemistry. Recently, the introduction of oxygen vacancies by the Mn oxides was found to be an effective strategy to further improve ORR activity, making it either similar or, in some cases, better than the Pt/C catalysts. [3] [4]

In this subsection, the experimental technique followed for the MnO_2 deposition on the cathodes will be presented. The procedure was thoroughly controlled to achieve consistent results across all treated cathodes.

The experimental setup used for the MnO_2 deposition on the cathodes was identical to the one described in subsection 3.1.2. This consistency ensured that the deposition process was carried out under controlled and reproducible conditions, allowing for reliable comparison and analysis of the results.

0,1 M $KMnO_4$ solution (4.74g $KMnO_4$ in 297ml H_2O) was used for each of the electrochemical depositions. The reference electrode employed was a saturated Ag/AgCl electrode, while a stainless steel 304 plate served as the counter electrode. In each deposition the cathodes functioned as the working electrodes.

Figure 18: *Cathode with the MnO_2 coating on the outer side*

The modification of the outer side of the cathode electrodes through the electrochemical deposition of MnO_2 is crucial for enhancing cell performance. MnO_2, known for its excellent electro-catalytic properties, significantly increases the rate of the oxygen reduction reaction (ORR). The ORR, a typically slow process, is one of the primary factors limiting the efficiency of microbial fuel cells. By coating the cathode with MnO_2, we utilized its catalytic capacity to accelerate the ORR, thereby mitigating one of the major inhibitors of cell performance. This enhancement not only improves the overall efficiency of the fuel cell, but also contributes to more stable and reliable operation. [5] [6]

3.4 Inoculation of the anode

The inoculation process is a crucial step, as it is during this phase that the biofilm forms on the anode. A total of 7 cycles were conducted to acclimate the anode of the MFCs using glucose as the organic substrate. The duration of each acclimation cycle was set at 1 day, during which chemical oxygen demand (COD), pH, and conductivity measurements were taken. Additionally, electrochemical tests like OCV, CV were obtained for each cycle to monitor the system's performance and stability.

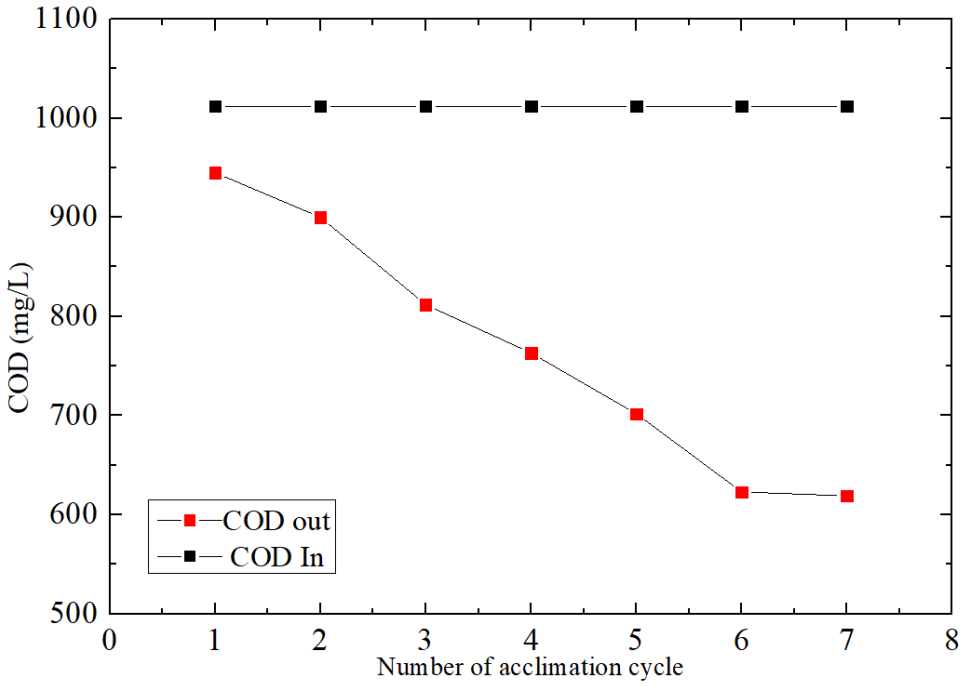

Figure 19: *Graph of COD measurements of the nutrient solution*

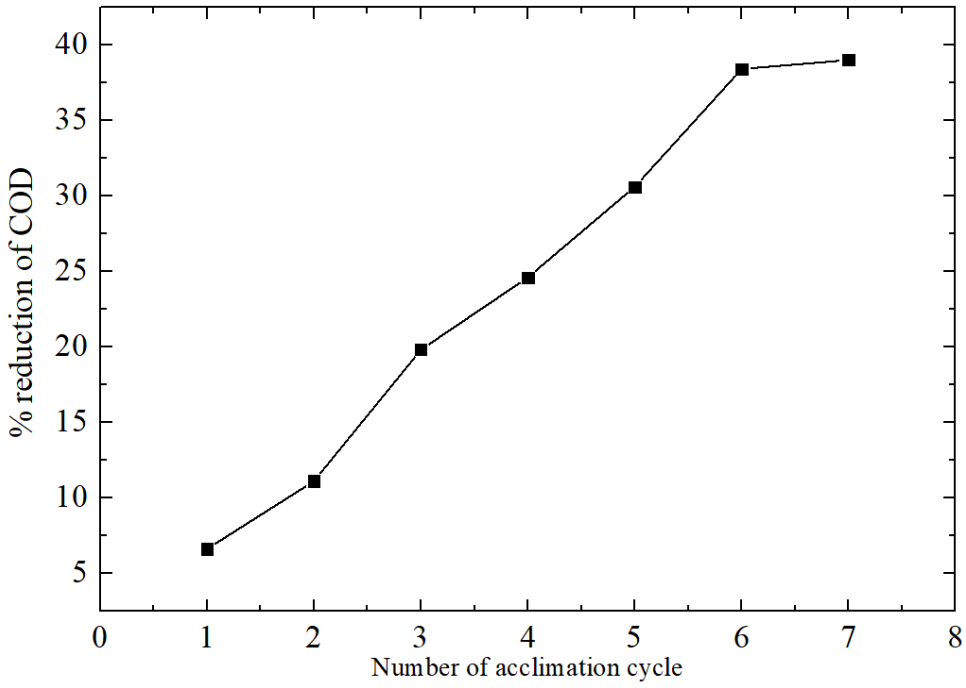

Figure 20: *Graph of % COD reduction of the nutrient solution*

Observation of the above diagrams indicates an increasing consumption of COD in the nutrient solution (initial concentration 1012 mg/L) over the 7 acclimation cycles, with consumption rates stabilizing between the 6th and 7th cycles. Specifically, as shown in Figure 20, the COD reduction progressively increases from 6.6% during the first acclimation cycle to 38.4% by the 7th cycle, after which it remains relatively constant at 39% during the final (7th) cycle. This stabilization in COD consumption signifies the full development of the E. coli biofilm on the anode and marks the conclusion of the acclimatization phase.

The results of the pH and conductivity measurements are displayed graphically in Figure 21 below and numerically in Table 2. pH measurements were conducted using a digital pH meter (WinLab Data Line pH-meter), while conductivity measurements were taken with a digital conductivity meter (CDM 83 Conductivity Meter), under temperature conditions ranging from 25 to 30 °C.

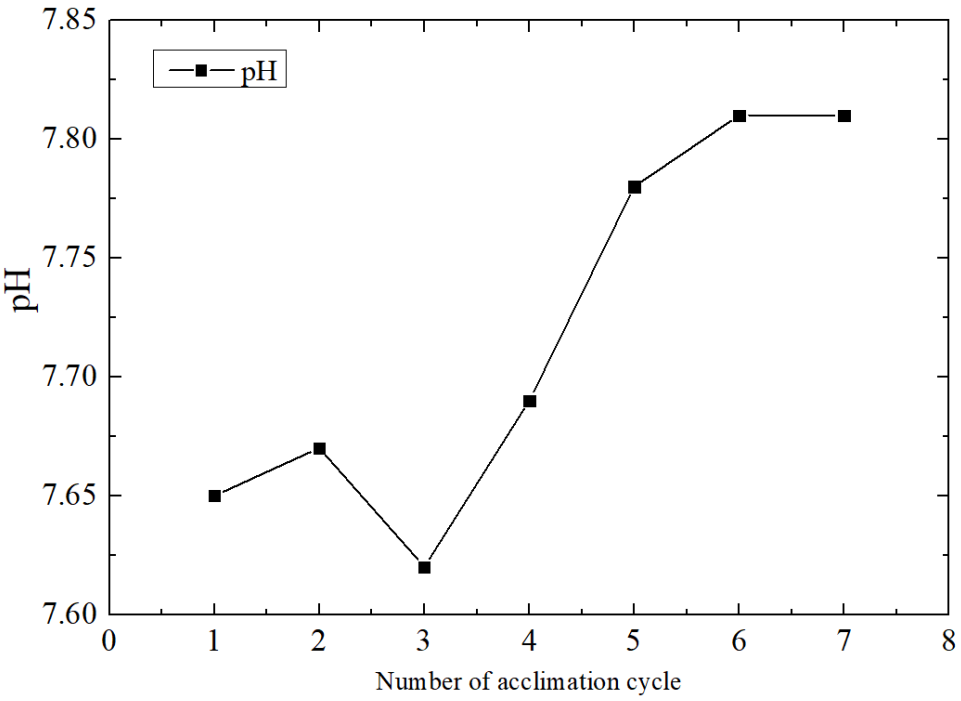

Figure 21: *pH graph during the inoculation process*

As observed from the above diagram, the pH for each acclimation cycle, is maintained near the neutral range, which is optimal for the growth and sustainability of the bacterial population. The initial pH of the anolyte solution before every acclimation cycle was 7.5.

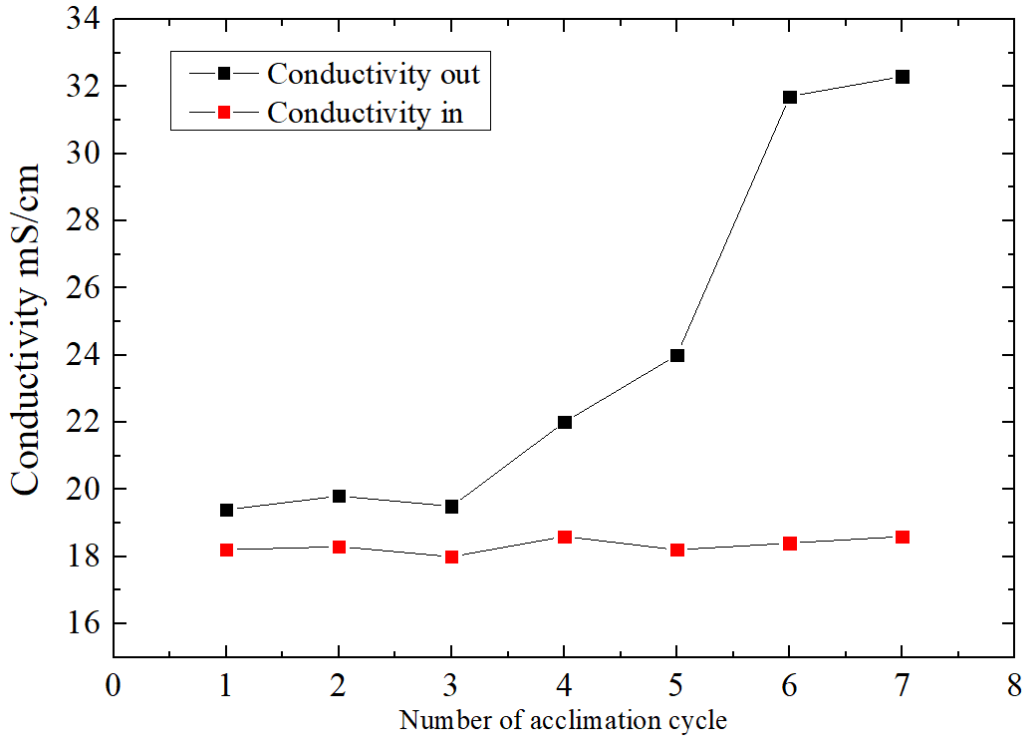

Figure 22: *Conductivity graph during the inoculation process*

Based on the above graphs and the conductivity data presented in Table 1, there is a noticeable overall increase in conductivity. This rise is primarily attributable to the protons (H+) generated at the anode. The marked increase in conductivity observed during the final acclimation cycles is likely due to the elevated proton concentration, considering the low rate of the oxygen reduction reaction (ORR).

Cycle number	**COD (mg/L) ± 4mg/L**			**pH (± 0,01)**		**Conductivity (mS/cm) ± 0,1 mS/cm**	
	Initial	Final	Reduction %	Initial	Final	Initial	Final
1	1012	945	6.6	7.50	7.65	18.2	19.4
2	1012	900	11.1	7.50	7.67	18.3	19.8
3	1012	812	19.8	7.50	7.62	18.0	19.5
4	1012	763	24.6	7.50	7.69	18.6	22
5	1012	702	30.6	7.50	7.78	18.2	24
6	1012	623	38.4	7.50	7.81	18.4	31.7
7	1012	619	39	7.50	7.81	18.6	32.3

Table 7: *Numeric presentation of COD, pH & conductivity measurements during acclimation cycle*

3.5 Waste treatment with blank ABS-CF cathode electrodes

Following the completion of the inoculation process, the microbial fuel cell (MFC) with cathodes chemically modified exclusively with NaOH treatment underwent three operating cycles, each running for one day. The results of the measurements taken during these operating cycles are detailed below.

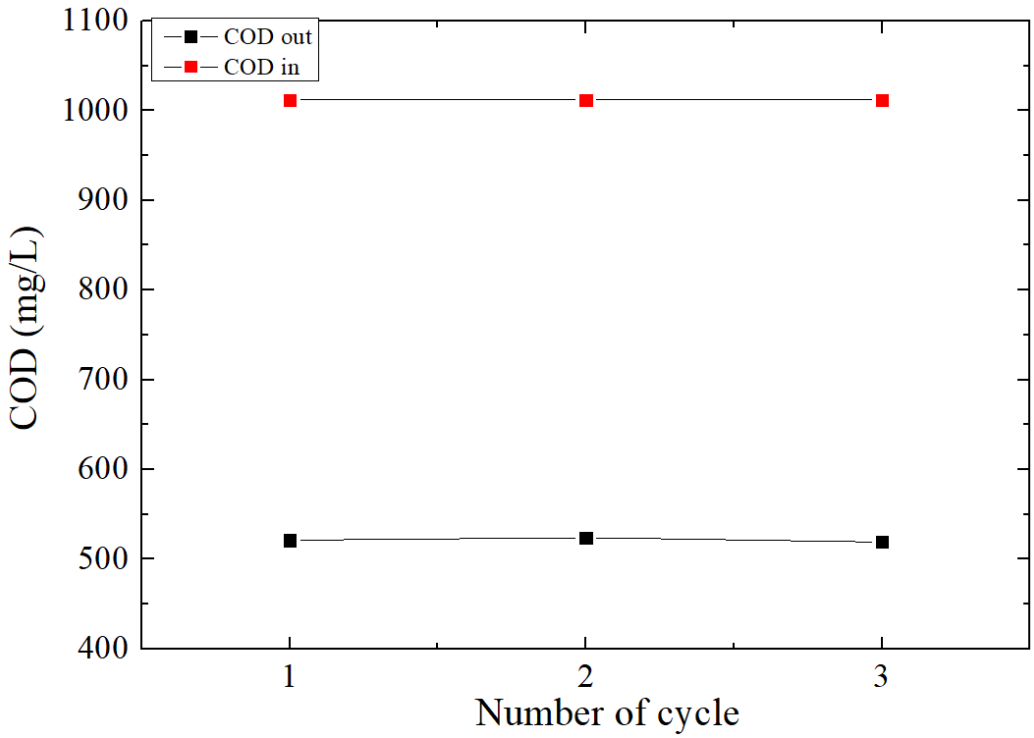

Figure 23: *COD diagram of the three operating cycles of the MFC with NaOH treated cathodes*

Cycle number	COD (mg/L) ± 4mg/L			pH (± 0,01)		Conductivity (mS/cm) ± 0,1 mS/cm	
	Initial	Final	Reduction %	Initial	Final	Initial	Final
1	1012	521	48.5	7.50	7.82	29.3	31.6
2	1012	524	48.2	7.50	7.84	29.1	33.2
3	1012	519	48.7	7.50	7.82	29.4	35

Table 8: *Numerical presentation of COD, pH & conductivity measurements during the treatment cycles of the MFC with NaOH treated cathodes*

The reduction rates for all three treatment steps are essentially identical as shown in Figure 23, with cycles 1, 2 and 3 achieving COD removal equal to 48.5%, 48.2%, 48.7% respectively.

From the pH and conductivity measurements, there is an increase in conductivity in the chamber. The buildup of positively charged ions, such as protons (H^+), can contribute to an increase in conductivity. Furthermore, a slight increase of pH is noticed possibly due to the fact that E. coli metabolism produces CO_2 as a byproduct. In aqueous solutions, CO_2 can form carbonic acid (H_2CO_3), which dissociates into bicarbonate ($HCO3^-$), and protons (H^+). $HCO3^-$ is a mild and weak alkali, thereby increasing the pH of the anolyte.

Polarization and power curves of the microbial fuel cell

A)

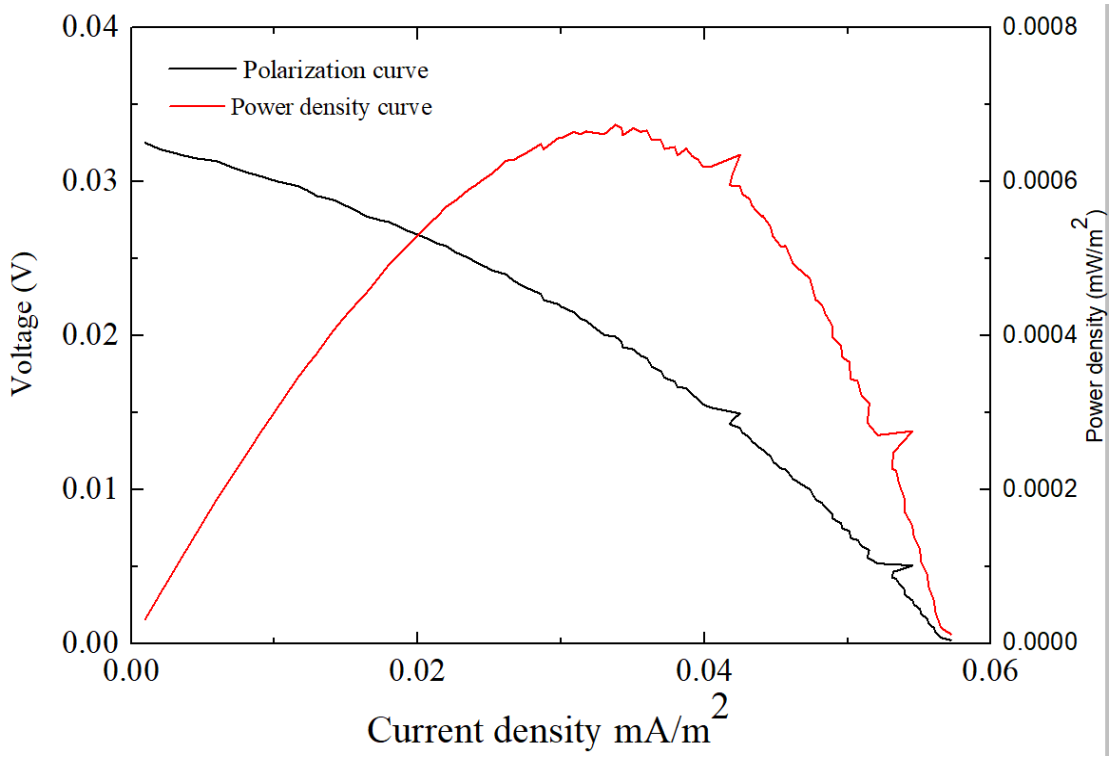

B)

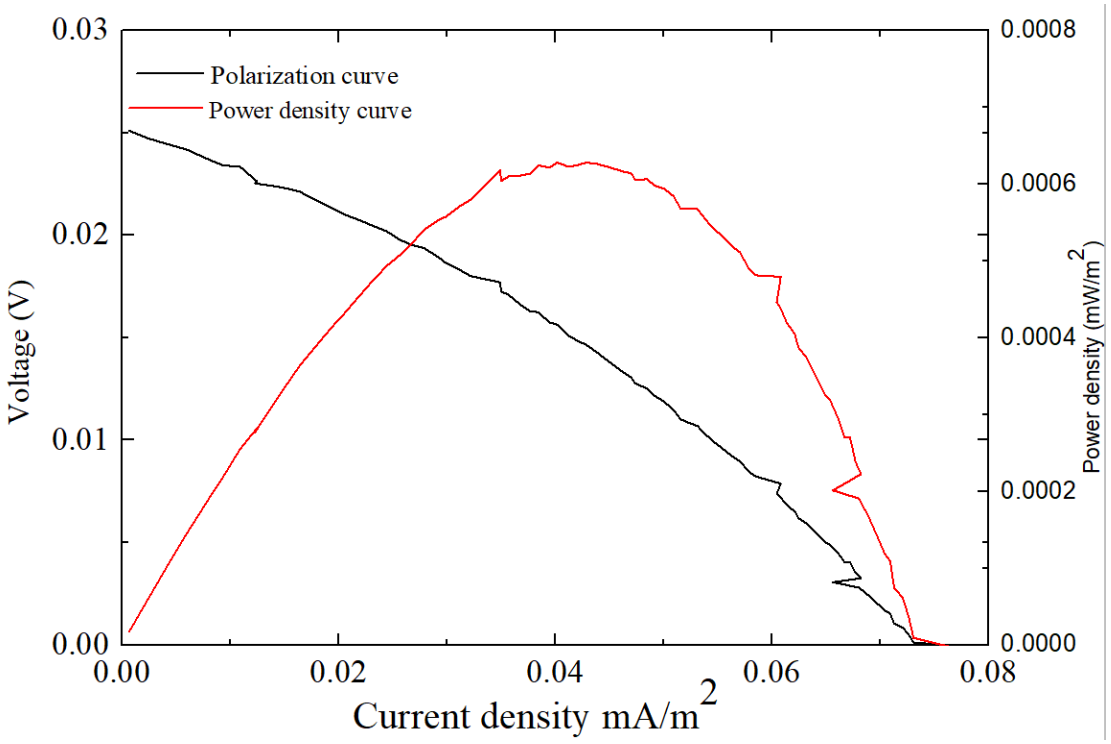
Polarization curve
Power density curve
Voltage (V)
Power density (mW/m2)
Current density mA/m2
0.03
0.02
0.01
0.00
0.0008
0.0006
0.0004
0.0002
0.0000
0.00
0.02
0.04
0.06
0.08

C)

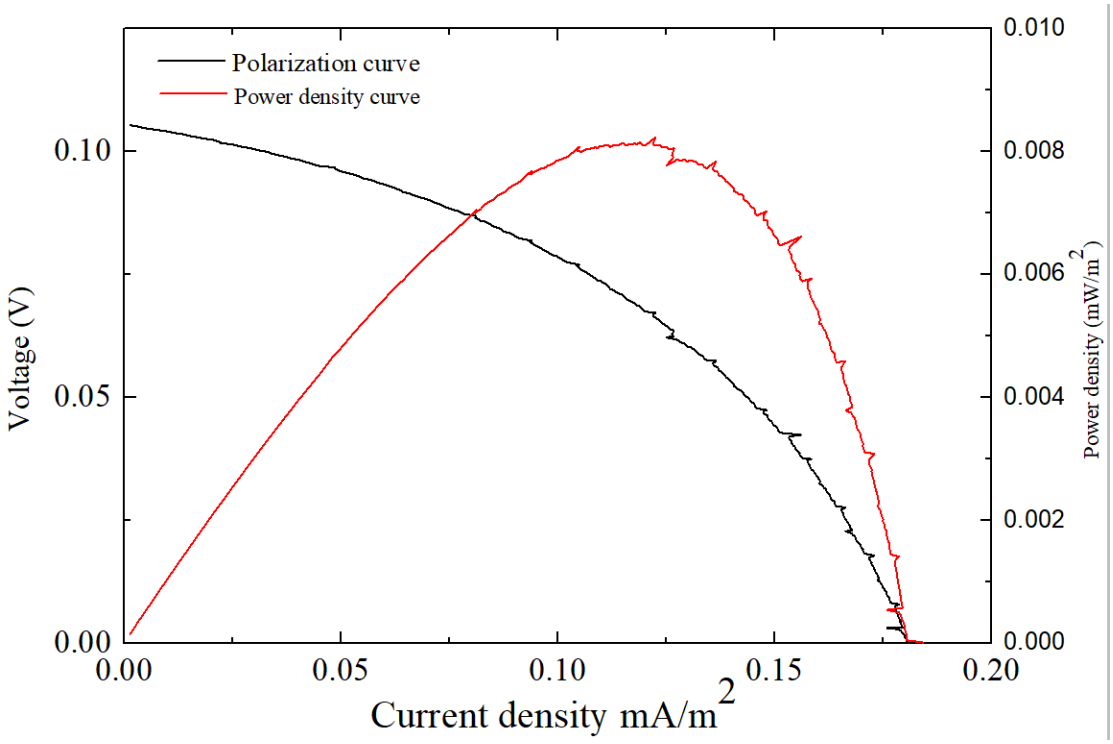
Polarization curve
Power density curve
Voltage (V)
Power density (mW/m2)
Current density mA/m2
0.10
0.05
0.00
0.010
0.008
0.006
0.004
0.002
0.000
0.00
0.05
0.10
0.15
0.20

Figure 24: *Polarization and power curves of 1st (A), 2nd (B) & 3rd (C) treatment cycles of the MFC with NaOH treated cathodes*

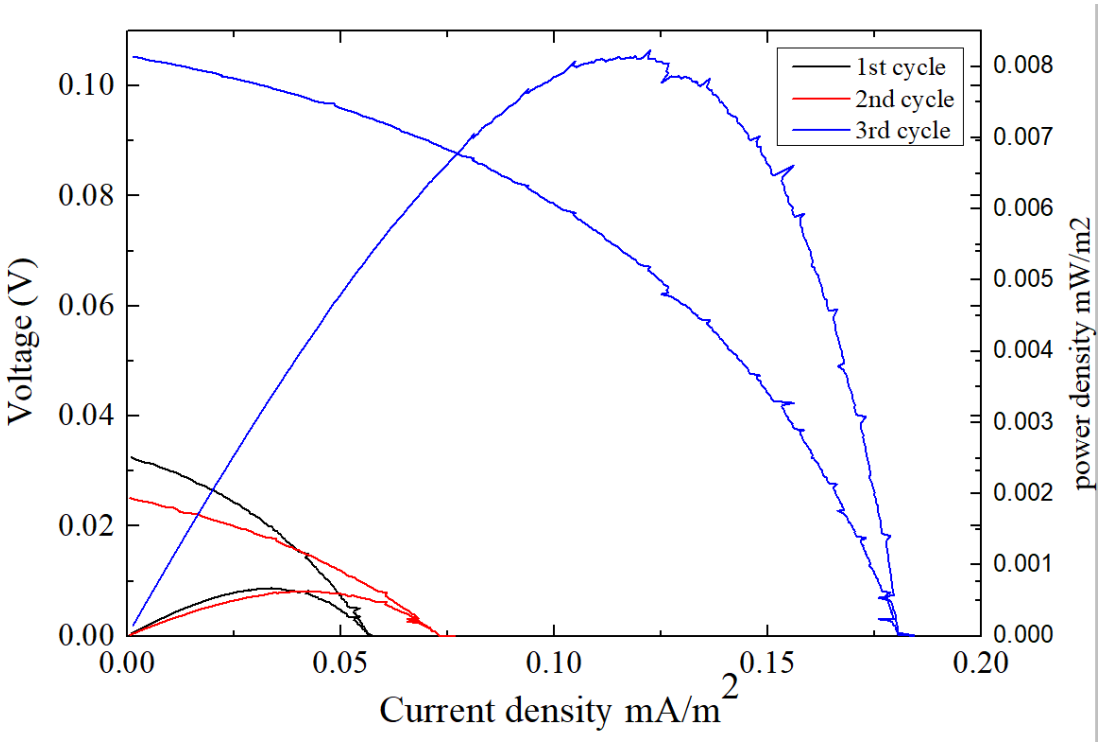

Figure 25: *Summarized presentation in a common diagram of the polarization & power curves of the 3 waste treatment cycles of the MFC with NaOH treated cathodes*

Number of cycle	OCV (V)	Maximum current value (mA)	Maximum current density value (mA/m^2)	Maximum power value (mW)	Maximum power density value (mW/m^2)
1	0,08	0,0008	0.060	0,00001	0.0007
2	0,10	0,001	0.072	0,0001	0.0006
3	0,07	0,002	0.079	0,0001	0.008

Table 9: *Numerical presentation of the results of electrochemical measurements in relation to the surface area of cathodes for the treatment cycle of glucose waste of the MFC with NaOH treated cathodes*

Both the diagrams and the table above show that the treatment cycle of glucose waste from the MFC with the uncoated cathode electrodes, is characterized by quite low power generation and low current intensity values. It is worth noting that the parabolic power curve in the 3rd cycle is not as symmetrical but leans towards the side of higher current intensity values. This indicates low internal resistance. In the region of higher current intensity values, where a sharp voltage drop is observed, polarization due to mass transfer dominates. This is due to the rate at which the compounds reach the surface of the anode and cathode electrodes, where the reactions take place. Furthermore the increase of the current and power density observed in the third cycle can be attributed to the fact that the cathode electrodes are stabilized and the losses are solely due to the internal resistance of the cell

The current density and the power density were calculated in relation to the surface of the cathodes.

3.6 Waste treatment with MnO_2 coated ABS-C cathode electrodes

After completing the treatment cycles of the glucose waste in the microbial fuel cell (MFC) using cathodes treated solely with NaOH, the experiment proceeded with three additional treatment cycles, utilizing MFCs equipped with MnO_2-coated cathode electrodes. The duration of each cycle was one day. Consistent with the protocol for the plain electrode treatment, during each cycle, open circuit voltage (OCV) measurements were conducted for the initial three hours of MFC operation. Subsequently, electrochemical measurements were performed to generate polarization and power curves.

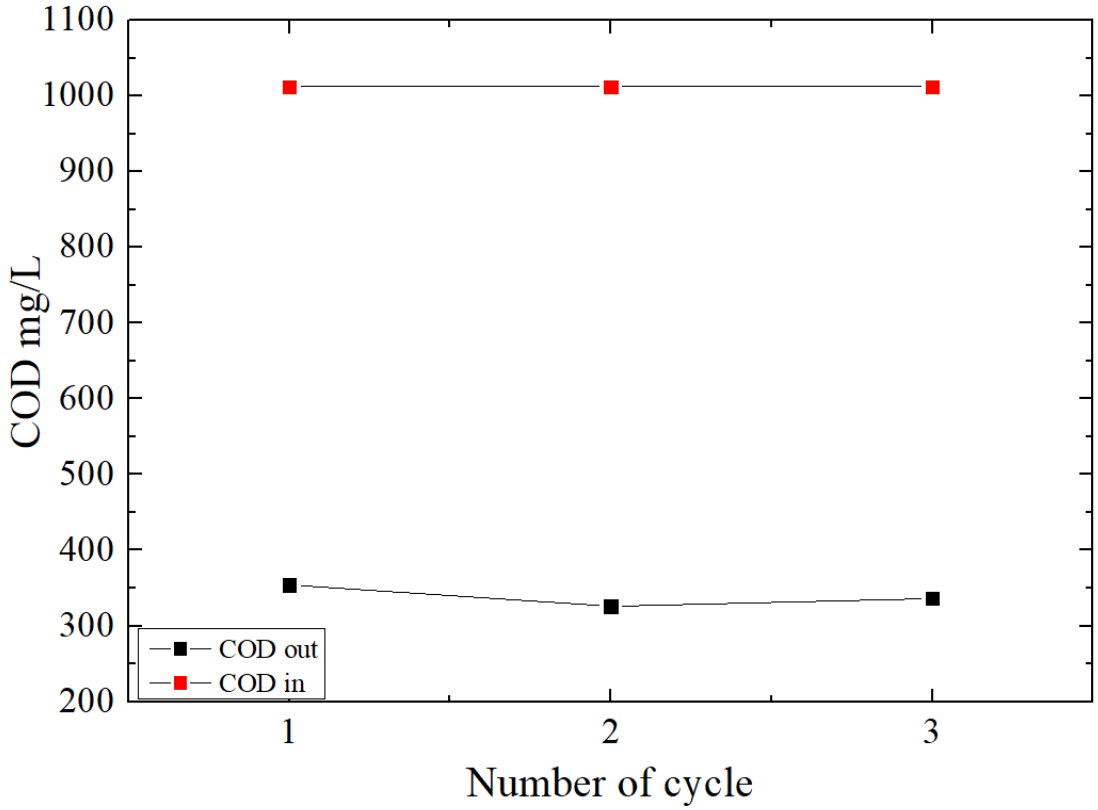

Figure 26: *COD diagram of the three operating cycles of the MFC of the MFC with NaOH treated - MnO_2 coated cathodes*

Cycle number	COD (mg/L) ± 4mg/L			pH (± 0,01)		Conductivity (mS/cm) ± 0,1 mS/cm	
	Initial	Final	Reduction %	Initial	Final	Initial	Final
1	1012	354	65.0	7.50	7.83	29.1	32.1
2	1012	319	68.4	7.50	7.85	28.9	34.2
3	1012	336	66.8	7.50	7.79	29.5	35.2

Table 10: *Numerical presentation of COD, pH & conductivity measurements during the treatment cycles of the MFC with NaOH treated cathodes*

The reduction rates for all three treatment steps are quite similar as shown in Table 8, with cycles 1, 2 and 3 achieving COD removal equal to 65.0%, 68.4%, 66.8% respectively.

The increase of conductivity and pH are again attributed to the presence of protons (H^+) and bicarbonate ($HCO3^-$) respectively, as explained in the previous subsection.

Polarization and power curves of the microbial fuel cell

A)

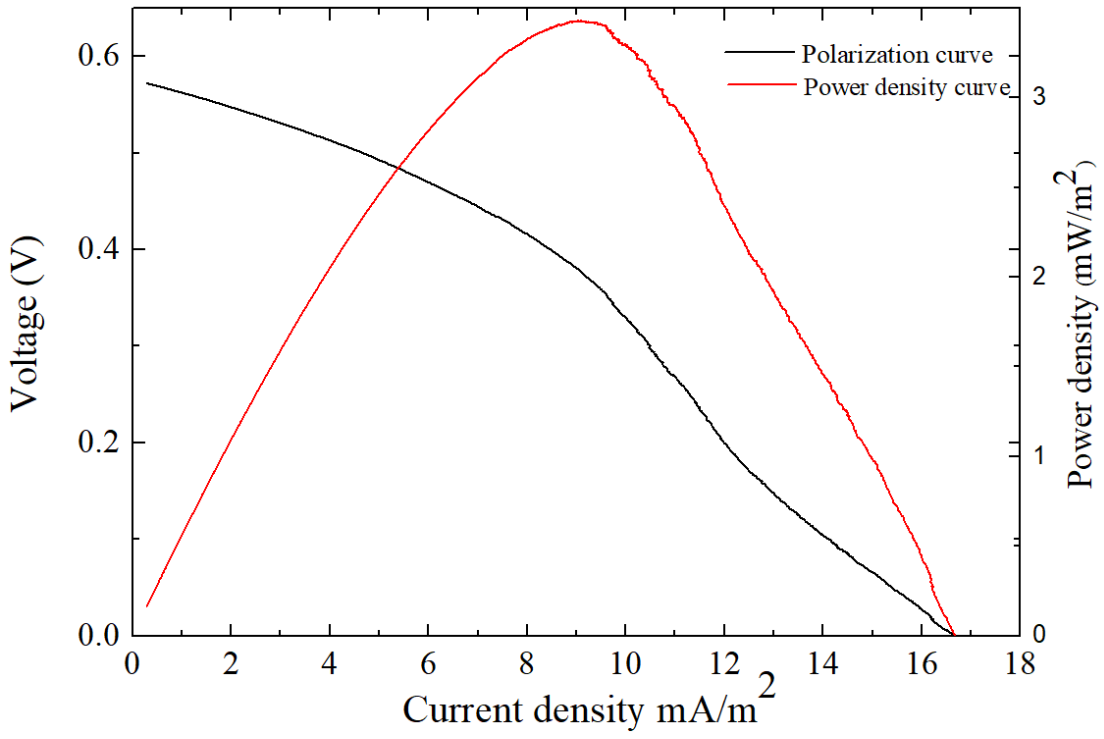

B)

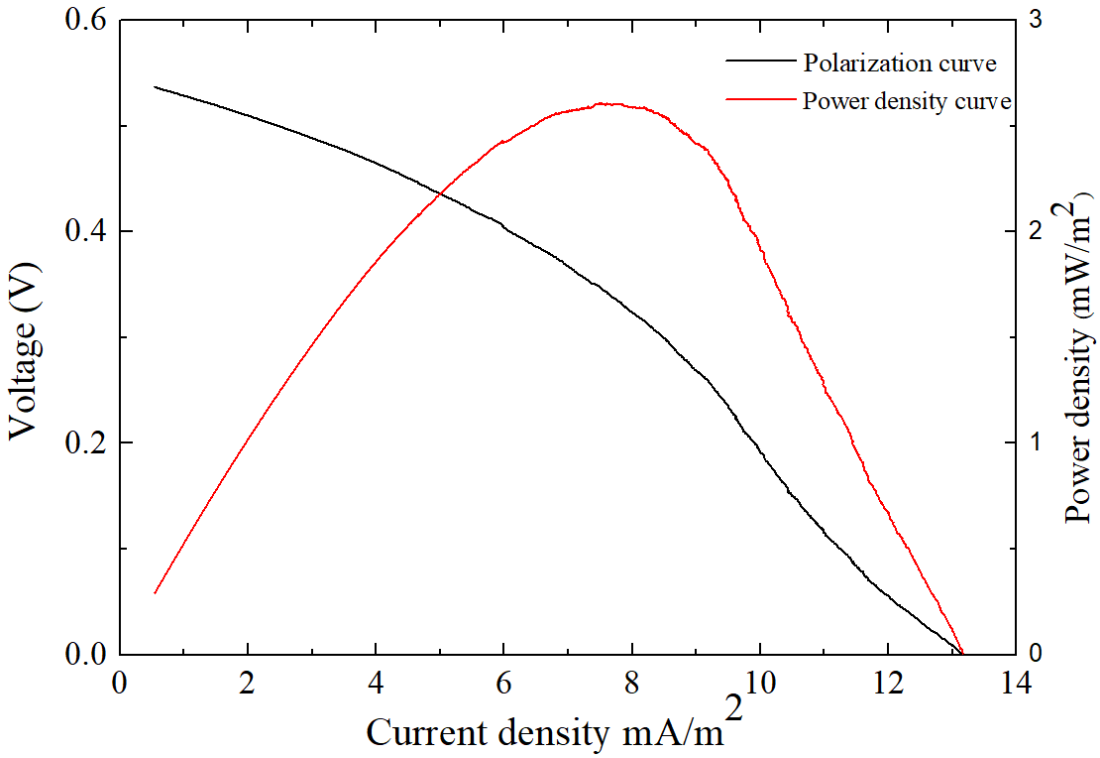
Polarization curve
Power density curve
Voltage (V)
Power density (mW/m2)
Current density mA/m2
0.0
0.2
0.4
0.6
0
1
2
3
0
2
4
6
8
10
12
14

C)

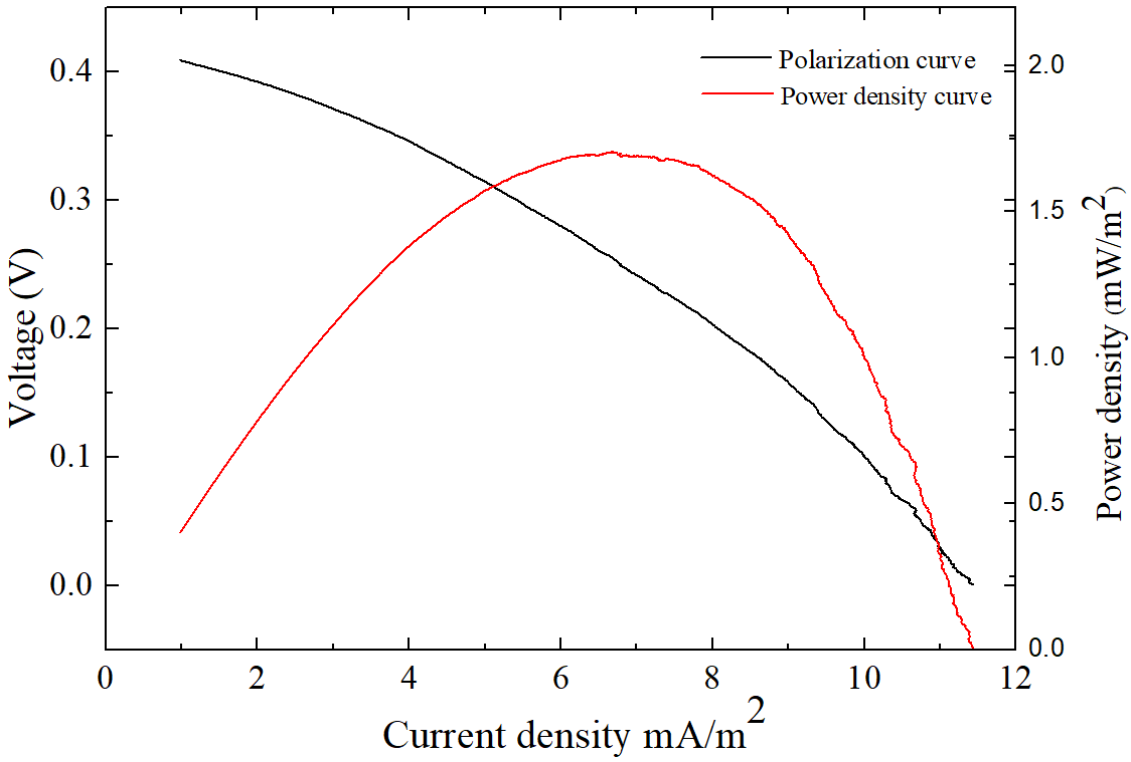
Polarization curve
Power density curve
Voltage (V)
Power density (mW/m2)
Current density mA/m2
0.0
0.1
0.2
0.3
0.4
0.0
0.5
1.0
1.5
2.0
0
2
4
6
8
10
12

Figure 26: *Polarization and power curves of 1st (A), 2nd (B) & 3rd (C) treatment cycles of the MFC with NaOH treated - MnO_2 coated cathodes*

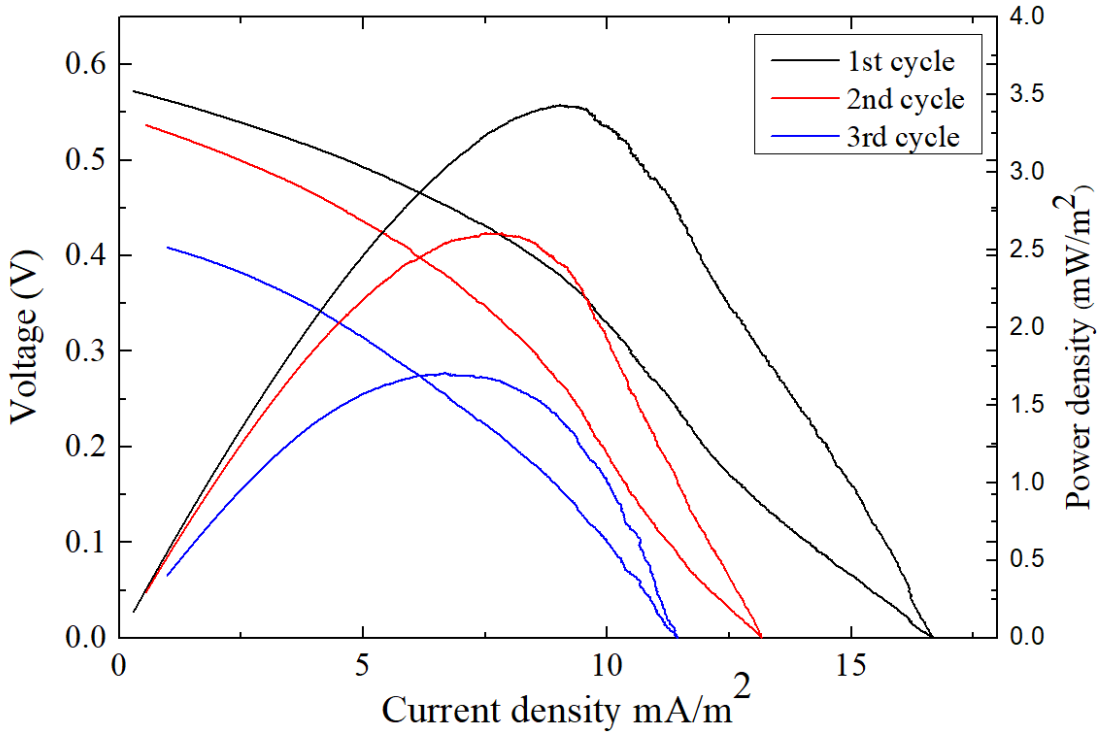

Figure 27: *Summarized presentation in a common diagram of the polarization & power curves of the 3 waste treatment cycles of the MFC with NaOH treated - MnO_2 coated cathodes*

Number of cycle	OCV (V)	Maximum current value (mA)	Maximum current density value (mA/m^2)	Maximum power value (mW)	Maximum power density value (mW/m^2)
1	0,50	0,23	16.59	0.048	3.42
2	0,49	0,18	13.09	0.036	2.60
3	0,19	0,19	11.34	0.024	1.70

Table 11: *Numerical presentation of the results of electrochemical measurements in relation to the surface area of cathodes for the treatment cycle of glucose waste of the MFC with NaOH treated - MnO_2 coated cathodes*

From the observation of the shape of the polarization curves of the 3 treatment cycles, the absence of losses due to mass transfer phenomena, which were dominant before the addition of MnO_2 electro-catalyst to the cathode electrode, is observed. MnO_2 enhances the presence of O_2 on the electrodes' surface, thus contributing to the acceleration of the ORR reaction. This is reflected in the significant increase in power generation and higher current intensity values, which are achieved from the very first cycle of treatment of the tanning waste from MFC with the coated cathode electrodes.

The decrease in power output and current intensity values generated by the MFC, from the first to the third operating cycles can be attributed to the MnO_2-coated cathodes experiencing fouling or degradation over time. The MnO_2coating can undergo electrochemical deactivation. Over time, the active sites on the MnO_2 surface may be blocked or altered, reducing its effectiveness in catalyzing the reduction reactions.

Nonetheless, the significant increase in power generation and current intensity observed during the treatment of the glucose waste demonstrates the importance of adding the catalyst to the cathode electrodes as a means to enhance the ORR reaction, which is generally a major inhibitor in achieving good performance of the MFCs.

3.7 Comparison of the different cathode electrodes

By comparing the results of the electrochemical and COD measurements obtained during the treatment of the glucose waste from the two MFCs, it is clear that significant increases in waste reduction, power generation and current intensity were achieved after cathodes' coating with MnO_2. In particular, based on the data in Tables 9 and 11, from the first treatment cycle with the modified electrodes, there is a remarkable increase in the maximum power density that can be delivered by the MFC ($3.42 mW/m^2$), which is about 4886 times higher than the corresponding one for the treatment cycle with the plain cathode electrodes ($7 \cdot 10^{-4} mW/m^2$). In the 2nd cycle, the maximum power density ($2.60 mW/m^2$) is about 4333 times higher than that in the case of the treatment cycle with the plain electrodes ($6 \cdot 10^{-4}$). Lastly, in the third cycle the maximum power density ($1.70 mW/m^2$) is about 213 times higher than that in the case of the treatment cycle with the plain cathode electrodes (0.008).

As far as waste treatment is considered both cells performed adequately, but again the MFC with NaOH treated - MnO_2 coated cathodes had an increase of approximately 20 units (~ 67%) compared to the MFC with only NaOH treated cathodes (~48%)

Despite the decrease of its power density, the MFC with the MnO_2 coated cathodes by far exceeded the efficiency both for waste treatment and of electrochemical performance, to the one that only had its cathodes treated with NaOH.

The presence of MnO_2 significantly enhanced the ORR reaction, which was a major limiting factor for the performance of the MFCs. In particular, the catalyst deposition on the ABS-C surface eliminated the mass transfer losses, as more oxygen vacancies were created on the electrode surface for oxygen reduction. MnO_2, due to its low cost and high efficiency in oxygen reduction, can be as a very good alternative to platinum (Pt), which is considered an ideal ORR catalyst, however its cost is rather high. [7]

3.8 Conclusions

The research presented in this thesis successfully demonstrates the design, fabrication, and performance evaluation of two single-chamber microbial fuel cells (MFCs) featuring innovative 3D-printed electrodes. The electrodes were made from an ABS polymer reinforced with carbon fibers, chosen for its cost-effectiveness and structural properties. The primary aim was to test the viability of this inexpensive, 3D-printed polymer material in achieving effective waste treatment and providing relatively good electrochemical results, particularly when enhanced with a MnO_2 coating.

Two configurations were tested: the first MFC with cathodes and anode treated solely with sodium hydroxide (NaOH), and the second with NaOH-treated electrodes further enhanced with a MnO_2 coating on the cathodes. Prior to the application of MnO_2, extensive testing confirmed that NaOH treatment was the most effective method for improving the bio-compatibility and electrochemical properties of the ABS-CF material.

The MFCs were subjected to three operational cycles after the inoculation of the anodes. The performance metrics, including open circuit voltage (OCV), polarization, and power curves, were monitored. The results unequivocally showed that the MFC with MnO_2-coated cathodes outperformed the MFC with plain NaOH-treated electrodes, demonstrating significantly better power generation and current intensity.

A noteworthy finding from the study was the substantial increase in chemical oxygen demand (COD) reduction achieved by the MFC with coated cathodes. This configuration improved COD reduction by 20 units, elevating the efficiency from 48% to 67%, compared to the MFC with plain electrodes. This enhancement in COD reduction highlights the superior capability of MnO_2-coated cathodes in facilitating more effective biodegradation of organic matter, thereby improving the overall wastewater treatment process.

The intricate 3D-printed designs of the electrodes played a crucial role in the enhanced performance by maximizing the surface area available for microbial attachment and electrochemical reactions. This structural optimization, combined with the catalytic effects of MnO_2, underscores the importance of electrode design and surface treatment in advancing MFC technology.

.

3.9 References for third chapter

[1] *H. Gao, D. Kaweesa, J. Moore, N. Meisel, Investigating the Impact of Acetone Vapor Smoothing on the Strength and Elongation of Printed ABS Parts, The journal of the Minerals, Metals & Materials Society,* ***2016****, 69*

[2] *Du A., Zhou Q. Zhibin W., Yang J., Kasteren J., Wang Y., Denitrogenation of acrylonitrile–butadiene–styrene copolymers using polyethylene glycol/hydroxides, Polymer Degradation and Stability,* ***2011****, 96, 870-874*

[3]*M. Browne, Z. Sofer, M. Pumera, Layered and two dimensional metal oxides for electrochemical energy conversion. Energy & Environmental Science,* ***2019****, 12, 10, 1039*

[4] *Y. Wang, J. Li, Z. Wei, Transition-metal-oxide-based catalysts for the oxygen reduction reaction, Journal of Material Chemistry,* ***2018****, 18*

[5] *Y. Hu, J. Wang, X. Jiang, Y Zheng, Facile chemical synthesis of nanoporous layered δ-MnO2 thin film for high-performance flexible electrochemical capacitors, Applied Surface Science,* ***2013****, 271, 193–201*

[6] *V.J. Mane, D.B. Malavekar, S.B. Ubale, V.C. Lokhande, C.D. Lokhande, Manganese dioxide thin films deposited by chemical bath and successive ionic layer adsorption and reaction deposition methods and their supercapacitive performance, Inorganic Chemistry Communications, 115,* ***2020****, 107853*

[7] *O. Lefebvre, W. K. Ooi, Z. Tang, Md. Abdullah-Al-Mamun, D. H.C. Chua, H. Y. Ng, Optimization of a Pt-free cathode suitable for practical applications of microbial fuel cells, Bioresource Technology,* ***2009****, 100, 20, 4907-4910*